

Channel Impulse Response Measurement for Characterizing The Ionosphere Communication Channel Over Java Island Indonesia

Varuliantor Dear¹, Iskandar Iskandar², Prayitno Abadi³, Cahyo Purnomo³, Asnawi Husin⁴, and Adit Kurniawan⁵

¹National Research and Innovation Agency

²Institut Teknologi Bandung

³National Research and Innovation Agency

⁴National Research and Innovation Agency (BRIN)

⁵Institut Teknologi Bandung

February 20, 2023

Abstract

For designing a digital High Frequency (HF) radio communication system in the skywave propagation mode, Delay spread and Doppler spread are the fundamental parameters of ionosphere channel characteristics that need to be known. Although the International Telecommunication Union (ITU) already provides general classification values for three different regions and conditions as a recommendation, the empirical Delay spread and Doppler spread values are still needed for an optimum design. As the role of HF communication in Indonesia is still important and its development technology is continued, the empirical data of ionosphere channel characteristics are also needed. However, the comprehensive empirical data of ionosphere channel characteristics over Indonesia is difficult to find. In this research, we developed an Ionosphere Channel Impulse Response (CIR) measurement system based on Software Defined Radio (SDR) with purpose to obtain the empirical values of Delay spread and Doppler spread. The measurement system is placed in Java Island Indonesia, which is in the Low latitude - Equatorial Ionosphere Anomaly (EIA) region. The specification of the system was determined based on the increased values of ITU parameters for low-latitude regions in order to be able to capture the possibility of higher values. The early measurement result shows slightly different values from ITU recommendation which is probably due to the EIA regions effect. This system is ready to collect further data to characterize the ionospheric communication channel comprehensively and investigate the space weather impact on HF communication systems.

1 **Channel Impulse Response Measurement for**
2 **Characterizing The Ionosphere Communication**
3 **Channel Over Java Island Indonesia**

4 **Varuliantor Dear ^{1,2}, Iskandar ¹, Prayitno Abadi³, Cahyo Purnomo⁴, Asnawi**
5 **Husin², and Adit Kurniawan¹**

6 ¹Sekolah Teknik Elektro dan Informatika - Institut Teknologi Bandung

7 ²Pusat Riset Antariksa - Badan Riset dan Inovasi Nasional

8 ³Pusat Riset Iklim dan Atmosfer - Badan Riset dan Inovasi Nasional

9 ⁴Stasiun Observasi Antariksa Atmosfer Sumedang - Badan Riset dan Inovasi Nasional

10 ¹Jl. Ganesa 20 Lebak Siliwangi, Bandung, Indonesia

11 ²Jl. Cisitua Sangkuriang, Bandung, Indonesia

12 ³Jl. Jl. Cisitua Sangkuriang, Bandung, Indonesia

13 ⁴Jl. Jl. Raya Bandung-Sumedang, Sumedang, Indonesia

14 **Key Points:**

- 15 • Development of ionosphere channel impulse response measurement system to ob-
16 tained the empirical data of Delay Spread and Doppler Spread
17 • The system is placed over Java island Indonesia which part of Low-Latitude-Equatorial
18 Ionosphere Anomaly region
19 • The system is ready to be used for collecting further data in order to character-
20 ize the ionospheric communication channel comprehensively

Corresponding author: Varuliantor Dear, varuliantor.dear@brin.go.id

Abstract

For designing a digital High Frequency (HF) radio communication system in the sky-wave propagation mode, Delay spread and Doppler spread are the fundamental parameters of ionosphere channel characteristics that need to be known. Although the International Telecommunication Union (ITU) already provides general classification values for three different regions and conditions as a recommendation, the empirical Delay spread and Doppler spread values are still needed for an optimum design. As the role of HF communication in Indonesia is still important and its development technology is continued, the empirical data of ionosphere channel characteristics are also needed. However, the comprehensive empirical data of ionosphere channel characteristics over Indonesia is difficult to find. In this research, we developed an Ionosphere Channel Impulse Response (CIR) measurement system based on Software Defined Radio (SDR) with purpose to obtain the empirical values of Delay spread and Doppler spread. The measurement system is placed in Java Island Indonesia, which is in the Low latitude - Equatorial Ionosphere Anomaly (EIA) region. The specification of the system was determined based on the increased values of ITU parameters for low-latitude regions in order to be able to capture the possibility of higher values. The early measurement result shows slightly different values from ITU recommendation which is probably due to the EIA regions effect. This system is ready to collect further data to characterize the ionospheric communication channel comprehensively and investigate the space weather impact on HF communication systems.

Plain Language Summary

Delay spread and Doppler spread are the fundamental parameter of a communication channel that should be known for designing the wireless digital communication system. Those parameters should also be known for designing the High Frequency (HF) digital communication system. Although International Telecommunication Union (ITU) already provides general values for three different locations and conditions, the empirical values of Delay spread and Doppler spread still need to be known for an optimum design. In this research, we reported the development of the ionospheric channel impulse response measurement system over Java Island Indonesia which is part of the low-latitude - Equatorial Ionosphere Anomaly (EIA) region. The purpose of the measurement system is to obtain the empirical Delay spread and Doppler Spread values with the specification of the system based on the increased values of ITU recommendation in order to be able to capture the possibility of higher values that could be occurred in the EIA region. Early measurement results show slightly different values from ITU recommendation which is probably due to the EIA region effect. This system is ready to use for collecting more data for characterizing the ionosphere communication channel comprehensively and for investigating the space weather impact on HF communication systems

1 Introduction

Ionosphere is one of the radio wave propagation mediums provided by nature for Beyond Line of Sight (BLOS) propagation in the High Frequency (HF) radio spectrum. Based on the advantages of the BLOS propagation, which are: (i) long-distance coverage area, (ii) minimum infrastructure requirement, and (iii) relatively low cost (Maslin, 1988), HF radio communication is used widely for military communication (Eliardsson et al., 2015) (Withington, 2020), post-disaster communication (Kitano et al., 2006), and regular communication with remote areas (Porte et al., 2018) (Abdullah et al., 2018). Those advantages are the basic reasons for the continuous development of HF Radio communication systems which transform into digital communication systems (Wang et al., 2018). However, for the development of an optimum digital communication systems, the fundamental information that should be known is the channel characteristic in terms of

71 Delay Spread and Doppler Spread parameters (Andersen et al, 1995). The Delay spread
72 is the spreading of the arrival time of radio wave multipath components through a chan-
73 nel, and the Doppler Spread is the spreading of the received frequency through the chan-
74 nel. Regarding to this important consideration, the characteristic of ionosphere chan-
75 nel should also be known for the design of HF digital communication system.

76 As part of space weather components, Ionosphere known as a dispersive commu-
77 nication channel which have temporal and spatial variations (Goodman, 2005). For gen-
78 eral reference in the design and test of HF digital modems, International Telecommu-
79 nication Union (ITU) already provides the ionospheric channel characteristic parame-
80 ters values as a recommendation (ITU, 2000). ITU generally classified the ionosphere
81 channel into three different regions and conditions for Delay spread and Doppler spread
82 channel parameters. The classification of three different regions of ITU are low latitude,
83 middle latitude, and high latitude. Meanwhile, the classification of three conditions of
84 the ionosphere are quiet, moderate, and disturbed. Those recommendation values are
85 helpful for basic digital communication design. However, some research shows that the
86 empirical data of channel characteristics are still needed in order to achieve the optimum
87 design for real world implementation (Ads et al., 2015) (Bergada et al., 2014) (Angling
88 et al., 1998). Therefore, for the development of HF digital communication in Indonesia,
89 the empirical data should also available. From the perspective of ionospheric physic mech-
90 anism, Indonesia is part of low latitude regions with some islands are rely on the Equa-
91 torial Ionospheric Anomaly (EIA) region. The Ionosphere in EIA regions known to have
92 higher electron density from other low-latitude regions due to the "fountain effect" mech-
93 anism (Duncan, 1960) and also a concentration of ionosphere scintillation. Therefore,
94 empirical data of ionosphere channel characteristics over Indonesia will also contribute
95 to the knowledge of the ionosphere behaviours in the low latitude-EIA regions as part
96 of space weather dissemination.

97 The Delay Spread and Doppler Spread could be obtained from the Channel Im-
98 pulse Response (CIR) measurement (Salous, 2013). To the best of our knowledge, the
99 research for measuring the channel impulse response in Indonesia is difficult to found,
100 except that has been done by Kurniawati et al.(2018). They investigated the statisti-
101 cal channel model of the ionosphere for 3044 km link between Surabaya and Merauke
102 from 5 days of measurement. Their research shows the distribution of Delay spread with
103 mean values in the range of 0–100 ms, 100–500 ms, and 500–1300 ms for 3 cluster multi-
104 hop modes namely 2F, 3F, and 4F. Those values are significantly higher compared to
105 the ITU recommendation. From our perspective, those higher values probably are not
106 defining the "pure" of ionosphere communication channel characteristics due to the fac-
107 tor of earth-surface reflections in the long haul multi-hop propagation mode. Therefore,
108 these results could not be suitable to be used for characterizing the basic ionosphere chan-
109 nel behaviours. Besides the possibility of influencing factors from the earth's surface re-
110 flection, the relative-short period of measurement are not enough to be use for three clas-
111 sification ionosphere conditions as given by ITU. For characterizing the ionosphere chan-
112 nel, this research could be improved by using different geometry of transmitter and re-
113 ceiver location alongside with its period of measurement. In this research, we develop
114 the ionosphere channel impulse response measurement system for low latitude region and
115 in Near Vertical Incidence Skywave (NVIS) propagation mode in order to obtain the em-
116 pirical Delay Spread and Doppler spread values for characterizing the ionosphere com-
117 munication channel. The development of the system is based on the Software Defined
118 Radio (SDR) platform and placed in Java island Indonesia which is rely on the crest re-
119 gion of Low Latitude-Equatorial Ionosphere Anomaly (EIA). To have a comprehensive
120 report, the structure of this paper is written as follows: in section 2 brief theory of chan-
121 nel impulse response measurement is described. In section 3, the design of the measure-
122 ment method and the determination of system parameters including the data post-processing
123 is described. In section 4 Result from operational testing and its discussion are described.
124 In the last section, the conclusion of this paper are given.

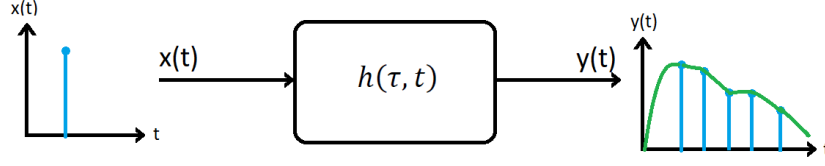


Figure 1. Linear time variant system model as representation of multipath channel.

125 **2 Channel Impulse Response Measurement**

126 A multipath wireless channel could be represented as the Linear Time-Variant model
 127 and could be characterized by its Channel Impulse Response (CIR) as illustrated in Fig-
 128 ure 1. The output of model $y(t)$ is the convolution of input $x(t)$ with the channel im-
 129 pulse response $h(t, \tau)$. From the channel impulse response, the information of multipath
 130 of radio wave propagations in the channel could be known in terms of its arrival time
 131 and its phase. For the ionosphere, the channel impulse response measurement could also
 132 be used for characterizations which needed in the design of digital communication sys-
 133 tem. The channel impulse response in the discrete form could be written as follows:

$$h(t, \tau) = \sum_{n=1}^N \alpha_n(t) e^{-j\varphi_n(t)} \delta(\tau - \tau_n(t)) \quad (1)$$

134 where α_n is the path loss and shadowing function, φ_n as the phase and Doppler func-
 135 tion, and δ is diract function for N number of multipath components. From $h(t, \tau)$, the
 136 scattering function $S(f, \tau)$ of a channel could be calculated using equation as follows:

$$S(f, \tau) = \int_{-\infty}^{\infty} R_{hh}(\Delta t, \tau) e^{-j2\phi f \Delta t} \partial \Delta t \quad (2)$$

138 where R_{hh} is the autocorrelation function of $h(t, \tau)$. The Scattering function $S(f, \tau)$ con-
 139 sists of two variable channels which are Power Delay Profile (PDP) and Doppler Spec-
 140 trum. Power Delay Profile is a function of time that describe the spreading of the time
 141 delay of the channel and could be expressed in equation as follows:

$$P(\tau) = \int_{-\infty}^{\infty} S(f, \tau) \partial f \quad (3)$$

142 For the spreading of frequency or Doppler spectrum, the calculation could done using
 143 equation as follows:

$$P(f) = \int_{-\infty}^{\infty} S(f, \tau) \partial \tau \quad (4)$$

144 From the spreading of the time delay or Delay spread and the spreading of Doppler fre-
 145 quency or Doppler spread, the Bandwidth coherence and the Time coherence of chan-
 146 nel could be obtained, respectively (Goldsmith, 2005). Bandwidth coherence and Time
 147 coherence are useful for determining the digital communication system parameters for
 148 an optimization.

149 **3 Methodology**

150 **3.1 System Design**

151 One of the popular techniques to measure the channel impulse response is a cor-
 152 relator channel sounder where firstly introduced by (Cox, 1975). In correlator channel
 153 sounder, an impulse signal which is represented by the Pseudo Random Bit Sequence

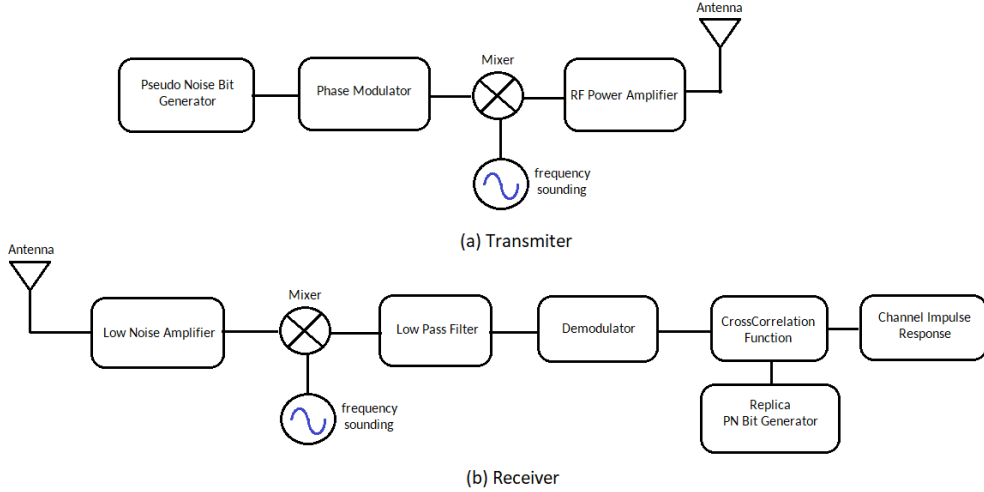


Figure 2. Correlator channel sounder block diagram for measuring the Ionospheric Channel Impulse Response.

154 (PRBS) is sent to the measured channel in order to be analyzed using its autocorrelation
 155 function on the receiver side. From the autocorrelation result, the number of gener-
 156 ated impulses in the channel could be obtained which represents the number of mul-
 157 tipath propagations in the channel. To avoid the mistaken calculation, the PRBS should
 158 have a good autocorrelation property. There are some PRBS that could be selected such
 159 as Maximum Length Sequence, Barker code, Gold code, and Kasami code (Salous, 2013).
 160

161 The block diagram of the correlator channel sounder for measuring the Ionosphere
 162 channel impulse response is shown in Figure 2. The transmitter block consists of Pseudo
 163 Noise (PN) code generator, Phase Modulator, Mixer, Radio Frequency Power Amplifier
 164 (RFPA), and Antenna. The PN code generator block generates the Pseudo Random Bit
 165 Sequence. In this study, the Maximum Length Sequence (MLS) bit was chosen. The PN
 166 bit sequence is then phase-modulated by the phase modulator block. The signal from
 167 the output of the modulator block is shifted from baseband frequency to the selected pass-
 168 band frequency in the mixer block. The magnitude of the signal output from the mixer
 169 block is increased in the RFPA block before being transmitted to the air by the antenna.

170 On the receiver side, the block diagram consists of Antenna, Low Noise Amplifier
 171 (LNA), Mixer, Low Pass Filter (LPF), Demodulator, and Cross-Correlation function to-
 172 gether with replica of the transmitted PN Bit Generator as part of the signal process-
 173 ing block. The magnitude of the received signal from the antenna is increased in the LNA
 174 block and then down-shifted to the baseband frequency by Mixer and Low Pass Filter
 175 block. The signal output from the Low Pass Filter block is then demodulated in the De-
 176 modulator block and continued to be processed in the cross-correlation function block
 177 using the replica of the transmitter PN bit sequences. The output of cross correlation
 178 function block is the channel impulse response which used to analyze the ionosphere chan-
 179 nel characteristics.

180 3.2 Determination of Software Defined Radio Parameters

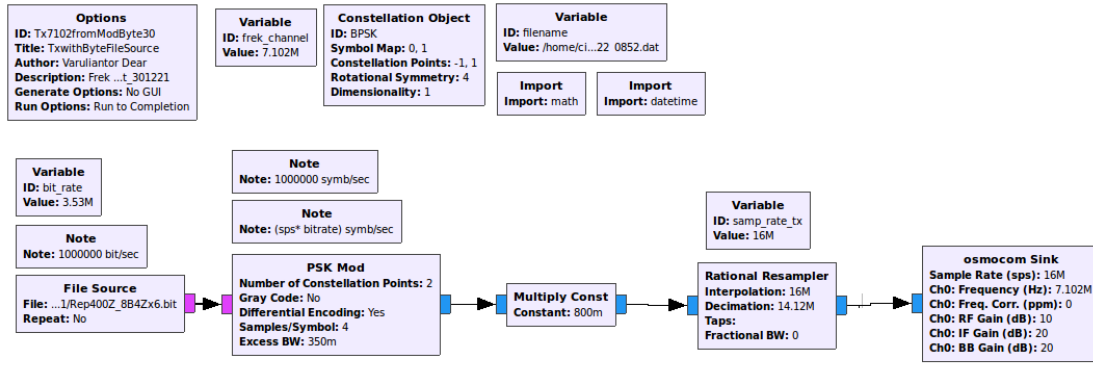
181 The temporal and spatial variation of the ionosphere are needed to be considered
 182 when determining the specification of the Ionosphere CIR measurement system. For mea-

183 suring the ionosphere channel characteristic over Java Island, Indonesia, the basic spec-
 184 ification of CIR measurement system could be chosen from ITU recommendation doc-
 185 ument for low latitude region as the minimum values. Those values are increased with
 186 the consideration that Java Island is part of the crest region of Equatorial Ionosphere
 187 Anomaly (EIA), which probably have higher values. The specification parameters of the
 188 ionosphere CIR measurement system are Time delay resolution (τ_{res}), Delay maximum
 189 (τ_{max}), and Maximum Doppler Frequency (fD_{max}). For this ionosphere CIR measure-
 190 ment system, the resolution of time delay is selected to be 5 times higher than the de-
 191 lay spread values from ITU recommendation for low latitude region in normal condition.
 192 The selected value was based on the consideration of the possibility of faster arrival time
 193 between each propagation path in the ionosphere. For the maximum of the time delay,
 194 the selected value is also 5 times higher than ITU Delay spread recommendation for low-
 195 latitude region with disturbed condition. The consideration of these selected values was
 196 from the possibility of the larger number of multi-hop radio wave propagation due to the
 197 occurrence of Equatorial Spread-F (ESF) which makes the ionosphere layer is in unsta-
 198 ble conditions (Abdu, 2001). For the Doppler frequency maximum, the selected value
 199 was 2 times higher than the value of Doppler Spread that given by ITU in low latitude
 200 region with disturbed condition. The Doppler frequency value could be increased more
 201 by using the sliding correlator technique in the post processing stage (Pirkl and Durgin,
 202 2008). Those specification parameters value will determine the parameter value of cor-
 203 relator channel sounder that used for this CIR measurement system design. In Table 1,
 204 the relation between target value for specification of ionosphere CIR measurement sys-
 205 tem with the ITU recommendation values are presented.

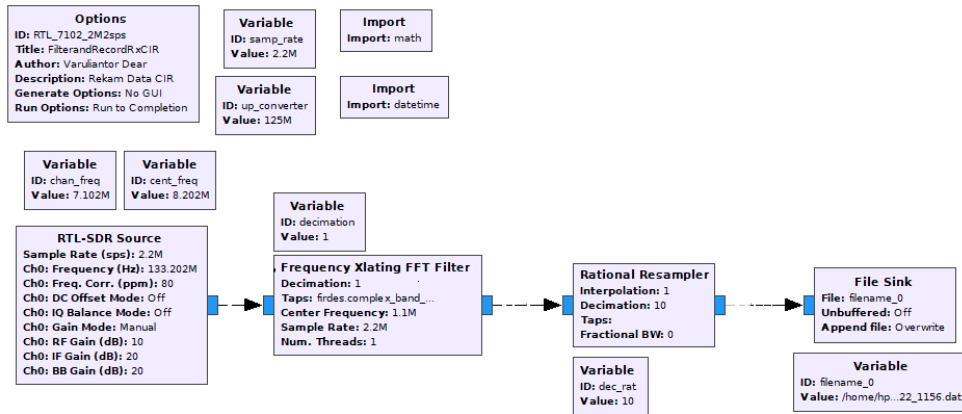
Table 1. Determination of ionosphere CIR specification target

Parameter	ITU Rec F.1487 Value	Target Value	Remark
Time delay resolution (τ_{res})	0.5 ms	0.1 ms	Delay Spread for low latitude with Quiet Condition
Max time delay (τ_{max})	6 ms	30 ms	Delay Spread for low latitude with Disturb Condition
Max Doppler frequency (fD_{max})	10 Hz	>10 Hz	Doppler Spread for low latitude with Disturb Condition

206 For optimum practical implementation, the determination of channel sounder pa-
 207 rameter values could use algorithm that provided by (Pirkl and Durgin, 2008). In this
 208 observation system, we determine the SDR parameters that will be used for the contin-
 209 uous operational system. The GNU Radio block diagram that used for implementing the
 210 correlator channel sounder is shown in Figure 3. In the transmitter side, file source block
 211 is used to read the prepared file which consists of PN bit sequence. The PN bit sequence
 212 from file source block are modulated by the Phase Shift Key (PSK) modulation block
 213 and resulting the modulated signal in the baseband spectrum. This modulated signal
 214 is re-sampled in the block rational resampler to meet the required sampling rate of Os-
 215 smocom sink block that used for shifting the signal to the selected sounding frequency
 216 while maintaining the bit rate. The Osmocom sink block is related with the specifica-
 217 tion of SDR hardware that used for transmitting the signal over the air. In this study
 218 HackRF one is used for the transmitter SDR hardware with sampling rate up to 20 Mega
 219 Symbols per Second (MSps) and frequency range 100 kHz to 6 GHz (Ossmann, 2016).
 220 From the configuration block diagram in GNU Radio and using an assumption that for



(a) Transmitter



(b) Receiver

Figure 3. Implementation of Correlator Channel Sounder in the GNU Radio software

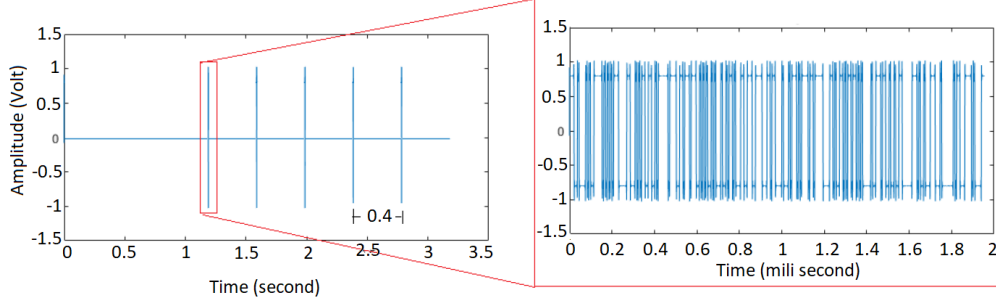


Figure 4. Waveform of sounding signal

221 one transmission is only consists of a single chip waveform, the determination of sam-
 222 pling rate values to meet the specification target in Table 1 could be use equation $Samplingrate =$
 223 $sps.bitrate$ where sps is the number of sample per symbol in modulator block diagram
 224 and bit rate is the number of bit that should be transmitted in one second which is equal
 225 to f_{chip} value. The modulation that use is Binary Phase Shift Keying (BPSK). There-
 226 fore, the values of sps is 2 which resulting the minimum of sampling rate is 20000 sam-
 227 ple per symbol. This value is below the specification of the SDR hardware and poten-
 228 tially could be implemented. Regarding to the target of time delay maximum and chip
 229 rate value, the bit PN sequence length could be determined using equation as follows:

$$230 \quad L = \tau_{max} f_{chip} = \frac{\tau_{max}}{\tau_{res}} \quad (5)$$

231 which resulting the length of PN bit sequence is 300. However, as the generation of Max-
 232 imum Length Sequence bit is in the form of shift register where the length value is based
 233 on powers of 2, the closest value is 255 which resulted from 2^8 . This selection of L will
 234 result τ_{max} is 25.5 ms. Although this value is different from the targeted delay maximum
 235 specification value, this value still higher compared to the ITU recommendation and could
 236 be accepted for the design of the ionosphere CIR measurement system.

237 The use of bit PN sequence with length 255 as the waveform for single sounding
 238 signal is already met with the specification target of CIR System. However, based on the
 239 consideration to the many possibilities of interference in the HF spectrum (Chen et al.,
 240 2010), the modification of sounding signal should be done with purpose to anticipate the
 241 interferences. Therefore, the sounding signal were modified by reshaping the waveform
 242 into 5 cluster of PN bit sequence with different time from each nearest neighbour of clus-
 243 ter PN bit is set to 0.4 second as shown in Figure 4. Beside for the redundancy purpose,
 244 the modification also intended for easier detection in the receiver side as the waveform
 245 contains more energy (Bole et al., 2014). This signal sounding modification is not chang-
 246 ing the chip rate value of the system.

247 For the implementation of the receiver block in the GNU Radio, the block diagram
 248 is simpler than the transmitter as it is intended for the post-processing technique. The
 249 block diagram are consist of RTL-SDR, Frequency Xlating FFT Filter, Rational Resam-
 250 pler, and File Sink Block. RTL-SDR and Frequency Xlating FFT Filter block are used
 251 for capture the passband signal and shifted to the baseband forms. The baseband sig-
 252 nal then resampler using rational resampler block to reduce the bandwidth of received
 253 signal up to 220 kHz which inherently reduced the size of the received signal without los-
 254 ing any information that needed for CIR calculation. At the File Sink block, the received
 255 signal were recorded for post-processing stage. The parameters of RTL SDR Block are
 256 related to the parameter of SDR hardware device which are sampling rate and frequency.
 257 In this study, the RTL-SDR hardware with chipset RTL2832U is used. The frequency

258 range and sampling rate maximum of RTL-SDR hardware is 50 MHz to 1,8 GHz and
 259 3,2 Msps, respectively (Laufer, 2014). Based on RTL-SDR device specification, the RTL-SDR
 260 could not capture the signal in the High Frequency spectrum. Therefore, the RTL SDR
 261 should be companion with Ham-It-Up Converter device which have function for direct
 262 sampling process. The combination with Ham-It-Up make RTL-SDR hardware able to
 263 capture the signal below 30 MHz (Drongowski, 2020). With this configuration, the value
 264 of frequency in the RTL-SDR block should also modified by adding the selected of sound-
 265 ing frequency with 125 MHz. The parameter values of GNU radio and its relation to achieved
 specification of CIR system are shown in Table 2.

Table 2. GNU Radio parameter values and achieved specification of CIR measurement system

Parameter	Value
f_{chip}	10000 bps
L_{PN}	255 bit
$Samp\ rate$	20000 symb/s
sps	2
τ_{res}	0.196 ms
τ_{max}	25.5 ms
fD_{max}	19.6 Hz

266

267

3.3 Additional Consideration for System Development

268

269

270

271

272

273

274

275

276

277

278

279

280

281

3.3.1 Determination of Transmitter and Receiver Locations

282

283

284

285

286

287

288

289

290

291

292

293

The transmitter and receiver locations for the CIR measurement are Pameungpeuk West Java (7.65S, 107.69E) and Bandung West Java (6.89 S, 107.59 E), respectively. The selection of those locations was firstly based on the available location and resources for long duration and continuous measurement purpose. The HF radio wave propagation between Pameungpeuk and Bandung already analyzed by (Jiyo, 2010) which conclude that the propagation of HF radio wave is only in the skywave propagation. The considerations of transmitter and receiver locations was also based on the availability of ionosonde instrument in Pameungpeuk which could provide the ionosphere density profile for confirmation and validation of the ionosphere conditions for this research. The map of transmitter and receiver locations are shown in Figure 6. The terrain between Bandung and Pameungpeuk is an east-west mountain chains which naturally blocking the ground wave propagation mode.

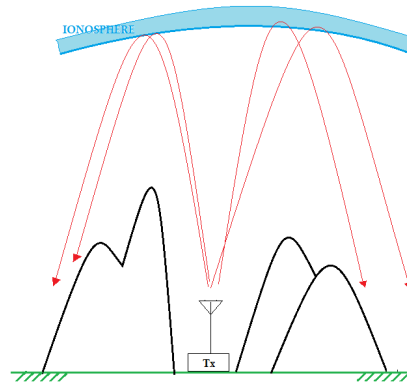


Figure 5. Illustration of Near Vertical Incident Skywave (NVIS) propagation mode

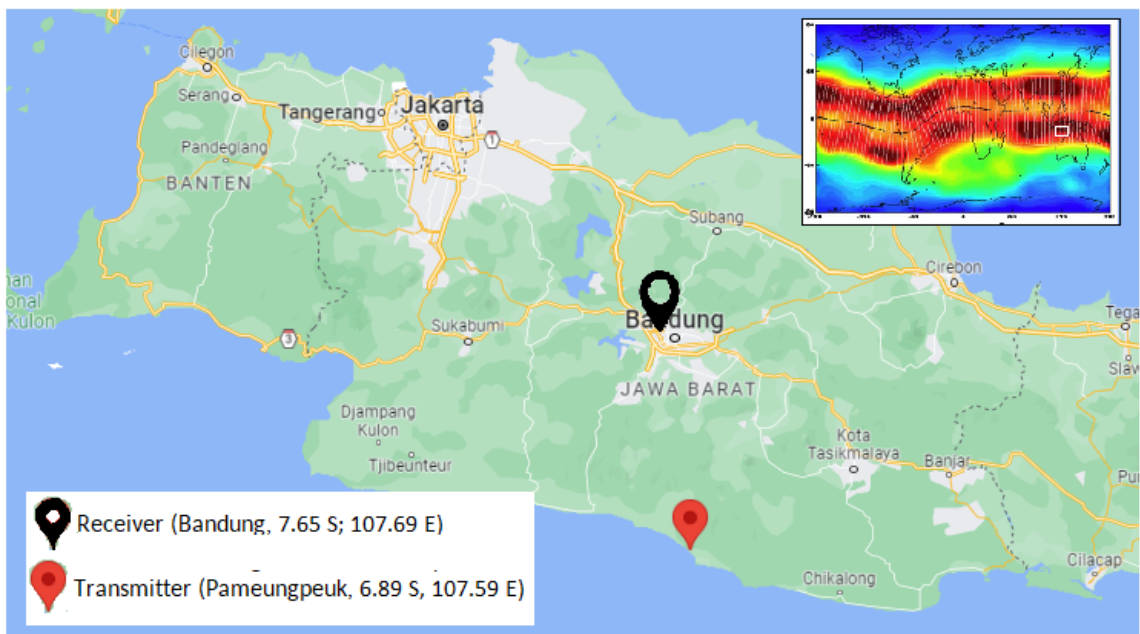


Figure 6. Location of Transmitter and Receiver Station

294

3.3.2 Selection of Sounding Frequency

295

296

297

298

299

300

301

302

303

304

305

306

307

308

309

310

311

312

313

314

The variation of ionosphere plasma density is affecting the frequency of radio wave that could be “reflected” to the earth’s surface. Therefore, to overcome this condition, the selection of the sounding frequency could be based on the frequency management method that usually use in HF radio communication plans (Maslin, 2017). In the frequency management method, the frequency was selected based on the variation of critical frequency of F layer (foF2) and minimum frequency (fmin) parameters from the ionosphere model. The frequency with the highest probability to appear between the foF2 and fmin values in the period of communication time is selected in order to guarantee the success of communication. In this study, the selection of the sounding frequency for CIR measurement is using Frequency management method based on the ionosphere model from Ionosphere Prediction System (IPS) Australia, namely Advance Stand Alone Prediction System (ASAPS) software (Commonwealth of Australia, Bureau of Meteorology, 2022). Model of foF2 and fmin were calculated for Bandung-Pameungpeuk circuits where its result shown in Figure 7. The models output from ASAPS are the Maximum Usable Frequency (MUF) and Absorption Lowest Frequency (ALF) which representing the foF2 and fmin values, respectively. From the model results, sounding frequency that selected in the CIR measurement are 3.453 MHz that used from 00:15 to 07:30 LT (UTC+7), and 7.102 MHz that used from 07:45 LT – 00:00 LT. The selection of those frequencies were also based on the legal permission to be use in the real world environment, as the author is member of amateur radio organization in Indonesia, namely ORARI.

315

3.3.3 Transmission Schedule and Measurement Timing

316

317

318

319

320

321

322

323

324

325

326

327

328

329

330

The measurement system is intended to be operated continuously and collect the result for a long period of measurement in the form of recording files. Therefore, the CIR measurement system needs to be set to work automatically and periodically for the effective and efficient of recorded file size. The CIR system is scheduled to work every 15 minutes for 24 hours a day with synchronization of sounding and recording time based on the internet reference time. However, due to the uncertainty of the time delay process from the SDR instrument (Ulversøy, 2010; Suksmono, 2013), a mismatch between the transmission and receiving time could occur. Therefore, to overcome this uncertainty of lag time, the scheduled time is added with time tolerance values both on the transmitter and receiver side. In the transmitter, the time for sounding the signal is set to start 3 seconds ahead of the recording signal in the receiver. On the receiver side, the recording time duration is extended three times from the sounding signal time duration in the transmitter. In practice, the scheduled transmission and receiving process is done using the Crontab-e functions that are already provided in UBUNTU operating system.

331

3.3.4 Link Budget Calculation

332

333

334

335

The output power of the transmission signal from HackRF one SDR device is only up to 0.03W (Great Scott Gadgets, 2021). To guarantee the transmitted signal could be arrived in the receiver antenna, the minimum required transmitted power could be calculated using equations as follows:

$$P_R = P_T + G_T + G_R + P_L \quad (6)$$

336

337

338

339

where P_R is the received Power (dBm), P_T is transmitted power (dBm), G_T is transmitted antenna gain (dBi), G_R is the received antenna gain (dBi), and P_L is the Path Loss (dB). For skywave propagation mode, P_L could be calculated using equation as follows:

$$P_L = L_a + L_{FSL} + L_g + L_p + L_q \quad (7)$$

340

341

where L_a is the absorption loss, L_g is ground loss, L_p is the polarization loss, L_q is the Loss from E layer, and L_{FSL} is the Free Space Loss. Regarding to McNamara (1991),

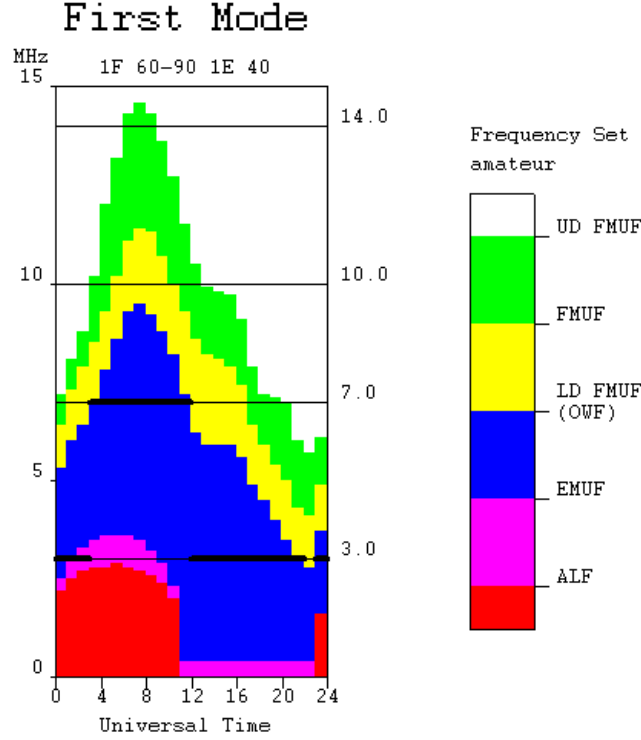


Figure 7. Result from ASAPS software for Bandung-Pameungpeuk circuits in December 2021. The selection of sounding frequency is based on the values between ALF and MUF

342 the maximum values of L_a , L_g , L_p , dan L_q is 20 dB, 3 dB, 6 dB and 9 dB, respectively.
 343 The value of L_{FSL} could be obtained using equation as follows:

$$L_{FSL} = 32,4 + 20\log(d) + 20\log(f) \quad (8)$$

344 where d is the distance of radio wave propagation path (km), and f is the frequency of
 345 radio wave (MHz). For NVIS propagation in this research, the distance (d) value is as-
 346 sumed to be 500 km and the frequency is 7 MHz. The distance value is obtained from
 347 two times values of average virtual height of F layer ($h'F$) which is 250 km. Using equa-
 348 tion (8) and (9) the Path Loss value is 103,28 dB. For the minimum of required trans-
 349 mitted power, the minimum of P_R values could be based on the RTL-SDR receiver sen-
 350 sitivity which is -139 dBm (HB9JAG, 2013)). From equation (7) the minimum required
 351 of P_T is 4.2 mW to guarantee the signal will be received in the receiver. In this CIR mea-
 352 surement system, the modul of Radio Frequency Power Amplifier (RFPA) and Low Pass
 353 Filter (LPF) from commercial HF radio transmitter Icom IC-718 are used as shown in
 354 topside of Figure 8. The average output power from this module is up to 100 Watt for
 355 Amplitude Modulation and Single Side Band transmission (Icom Inc., 2015) which enough
 356 to be used in this system although some loss from cables and connector occurred. To-
 357 gether with the use of RFPA and LPF module in the transmitter site, the HF Broad band
 358 Folded Dipole Antenna is used for an effective signal transmission over the air. At the
 359 receiver site, the similar 30 meter long wire antenna is also use but with simpler receiver
 360 hardware device as shown in bottom side of Figure 8. The specification of the hardware
 361 that used in the CIR measurement system are described in Table 3.



(a) Computer (b) HackRF One SDR (c) ICOM IC-718 (d) Power Supply (e) HF Broadband Folded Dipole Antenna

Transmitter Site



(a) RTL-SDR with Hamit-Up converter (b) Computer (c) HF Broadband Folded Dipole Antenna

Receiver Site

Figure 8. Hardware device for transmitter site (topside) and receiver site (bottom side)

Table 3. Hardware Device and Specification of Ionosphere CIR measurement system

Device	Transmitter	Receiver
SDR Hardware	HackRF One 20 Msps	RTL-SDR with HamitUp 3.2 Msps
SDR Software	GNU Radio 3.7	GNU Radio 3.7
Antenna	ICOM AH-710 (3-30 MHz)	ICOM AH-710 (3-30 MHz)
Personal Computer	Core i3 with UBUNTU 16.04	Core i3 UBUNTU 18.06
RF Power Amplifier	Icom IC-718 <i>Power</i> up to 100 Watt	none

3.4 Data Post Processing

The recorded of the received signal $r(t)$ are in the form of complex values which could be written as follows:

$$rt = s(t) * h(t) \quad (9)$$

where $s(t)$ is the transmitted signal and $h(t)$ is the ionosphere channel impulse response. To obtain the ionosphere channel impulse response from the recorded signal, the cross-correlation calculation between $r(t)$ and $s(t)$ could be done using equation as follows:

$$h(\tau) = r_{sr}(\tau) = \int_{-\infty}^{\infty} s(t)r(\tau + t)\partial\tau \quad (10)$$

where $r_{sr}(\tau)$ is the cross-correlation between $s(t)$ and $r(t)$. According to (Sakar, 2003), the obtained of ionospheric channel impulse response are representing the Power Delay Profile (PDP) that can be written in equation (1). From Power Delay Profile, the calculation of the root mean square (r.m.s) of time delay or delay spread could be done using equation as follows:

$$\tau_{rms} = \sqrt{\frac{\sum_i |\alpha|^2 (\tau_i - (\frac{\sum_i |\alpha|^2 \tau_i}{\sum_i |\alpha|^2}))^2}{\sum_i |\alpha|^2}} \quad (11)$$

where τ_i is the time delay for each path i . For the calculation of the Doppler spread, equation (8) could be use to calculate the Doppler Spectrum $S(f)$ using equation as follows:

$$S(f) = \int_{-\infty}^{\infty} r_{hh}(\Delta t, \tau) e^{-j2\phi f \Delta t} \partial \Delta \tau \quad (12)$$

where r_{hh} is the autocorrelation of ionosphere channel impulse response. From the half of Doppler spectrum values, the Doppler spread could be determined.

4 Result From Operational Testing

An example result of the recorded received signal from single measurement is shown in Figure 9. This received signal will be used in the post-processing stage to obtain the ionosphere channel impulse response and its analysis. The received signal is shown in the form of time domain and frequency domain in the Intermediate Frequency (IF) spectrum. From the time-domain graph in Figure 9, the target of the received signal that will be used for the post-processing stage could not be seen clearly. However, in the frequency domain, the targeted of the received signal could be seen clearly which appears between 1 kHz to 3 kHz and starting from the second and ending at the fifth second of the recording time. The duration of the targeted received signal is matched with the duration of transmitted sounding signal as shown in Figure 4. From the received signal in Figure 9, it can be seen also that the receiver was able to receive another signal with different frequencies. During the measurement periods, some signals with significant power,

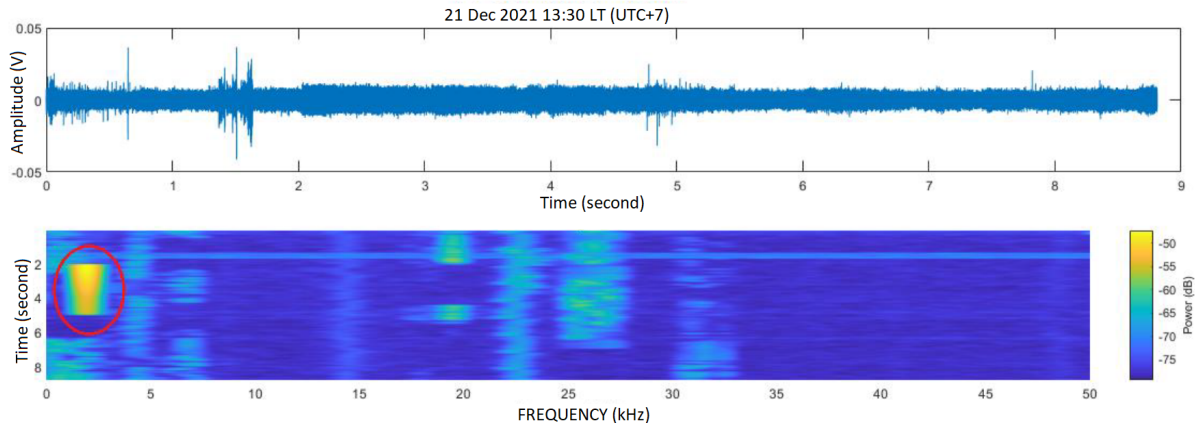


Figure 9. The received signal on 21 December 2021 at 13:30 LT (GMT+7). The targeted of the received sounding signal is between the 2nd and 5th second in the range of 1 kHz to 2.5 kHz at the Intermediate Frequency spectrum. The recorded signal also shows other received signals in different range of frequencies with significant power, bandwidth, and duration.

bandwidth, and durations in the frequencies 1 kHz, 4 kHz, 7 kHz, 15 kHz, 23 kHz, 26 kHz, and 32 kHz are also recorded. Those signals are representing another signal with different carrier frequency where its source could not be exactly identified as it could be from an amateur radio signal or broadcast station. In the range of the selected sounding frequency and in the transmission time period, it can be seen also there are some interference signals from the neighbour frequencies which could be influencing the post-processing of the received signal. From the Figure, it can be seen also that before the sounding signal was received, a wide band signal with a short period transmission time was received. This impulsive signal interference types is possible to be occurred in the same time of transmission sounding signal in the future and could not be avoided. Therefore, the redundancy technique by using 5 clusters of repeated PN bit sequences that are already explained in the methodology section is used for a mitigation.

From the received signal in Figure 9, the result of ionospheric channel impulse response calculation are shown in Figure 10. The observed of channel impulse response are consist of five cluster of Power Delay Profile with time different between the nearest neighbour cluster is around 0.4 second which follows the transmitted sounding signal as shown in Figure 4. From Figure 10b it can be seen the different number and magnitude of received impulse signal for each group. Those results show the system can captured the variation of the ionosphere channel in term of its propagation time delay. The smallest time delay that captured is 0.22 ms (CIR #1) and the highest time delay is 1.8 ms (CIR #3). Based on the specification of time delay resolution and the smallest value of delay spread given by ITU, the measurement system shows its capability to capture the ionosphere channel variation according to its specification designed. However, based on the values of the maximum of time delay that obtained in this result, the design of CIR systems could not confirm it's capabilities, yet. This condition could be occurred due to the quiet condition of ionosphere during the observation time. In Figure 11, ionogram from ionosonde during observation of CIR is shown to confirm the ionosphere conditions from its traces. It can be seen that the trace of the echo signal has clear and smooth shape without a small cusp or twist, and not spreading in time either in frequency which indicate the normal of ionosphere layers (Munro, 1953) (Munro and Heisler, 1958). From the confirmation of the quiet ionosphere condition in Figure 11, the maximum of time delay that obtained are reasonable and could be accepted.

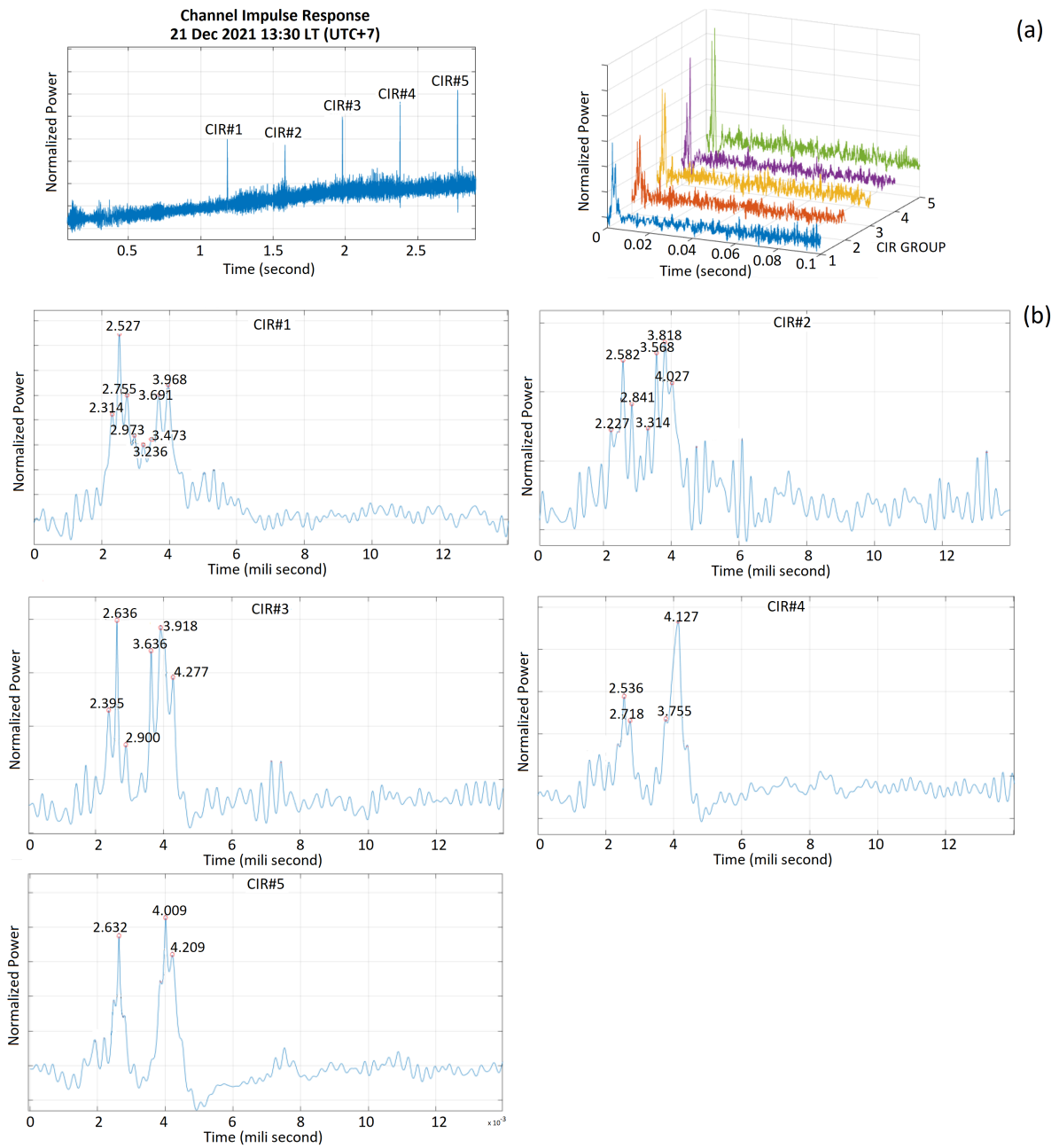


Figure 10. Ionospheric Channel Impulse Response result from 21st December 2021 at 13:30 LT (UTC+7). Five group of CIR was observed with two impulse cluster with different number and magnitude.

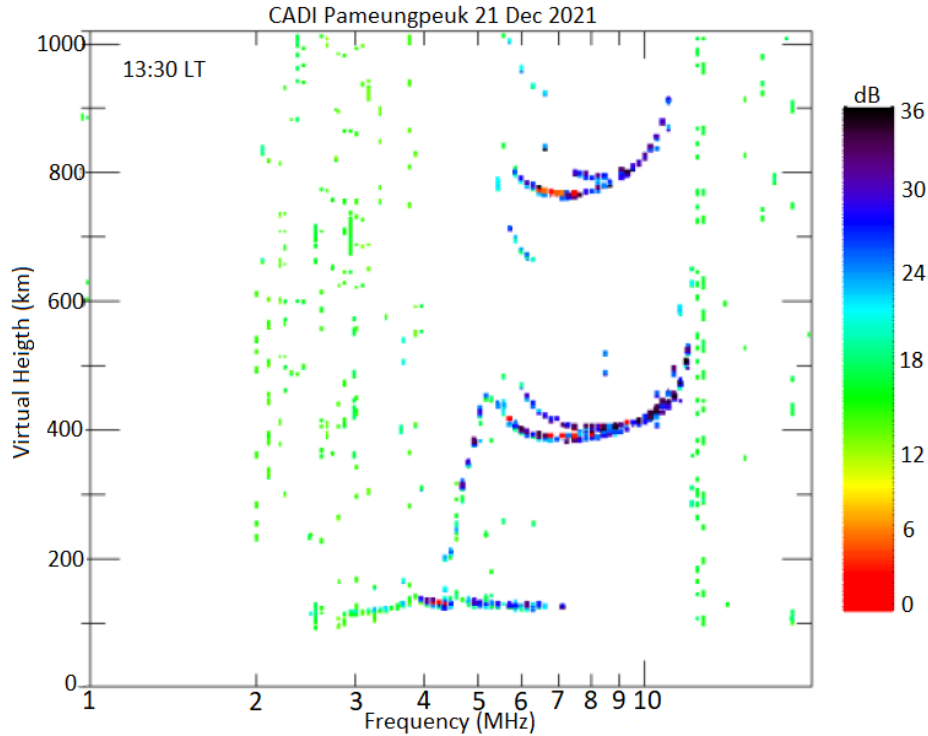


Figure 11. Ionogram from ionosonde at Pameungpeuk during the observation of CIR at 13:30 LT (UTC+7) on 21st December 2021 for the confirmation the stability and normal ionosphere conditions.

422 From ionogram in Figure 11, it can be seen also that E Sporadic layer were appeared
 423 with critical frequencies (f_oE_s) values more than 7 MHz where the CIR sounding frequency
 424 is used. The impact of the existence of E Sporadic layer was captured in the 5 group of
 425 CIR measurement result. In each of CIR group, we can see two cluster of impulse with
 426 variate amplitude (Figure 10). The presences of E Sporadic layer in the received impulse
 427 could be confirmed from its apparent distance calculation compared to the distance be-
 428 tween virtual height of F layer and E layer. The different time between first impulse of
 429 second cluster and last impulse of first cluster in CIR #1 is $3.691 - 2.314 = 1.377$ ms. There-
 430 fore, the calculation of apparent distance travelling time between those two impulse clus-
 431 ters using speed of light c is 300000 km/s is 413.1 km. Half of this values is the estima-
 432 tion of different virtual height of E ($h'E$) and F ($h'F$) layers which is around 200 km. In
 433 this system, the absolute time delay that could be used for calculating the distance of
 434 the propagation path was not measured for the simplicity and the low cost of the designed
 435 system.

436 Early result measurement in the form of variation of Time Delay and Doppler frequ-
 437 ency with their distributions from 15th December 2021 to 21st December 2022 are shown
 438 in Figure 12. Figure 12a show the root mean square (r.m.s) of time delay with its dis-
 439 tribution. The r.m.s of time delay for 7 days observation is fluctuated with in range be-
 440 tween 0 to $1,3$ ms. This fluctuation show the ionosphere channel is change randomly. To
 441 obtained the general value of Delay spread, the statistical analysis approach of root mean
 442 square time delay could be done by using its distribution. From the distribution in Figure
 443 12a, it can be seen that the mean of r.m.s delay spread is 4.627 ms and follows the
 444 Rayleigh distribution with the Delay spread values are tend to have more occurrence be-
 445 low its mean values. This one-week Delay Spread measurement values is different 0.373

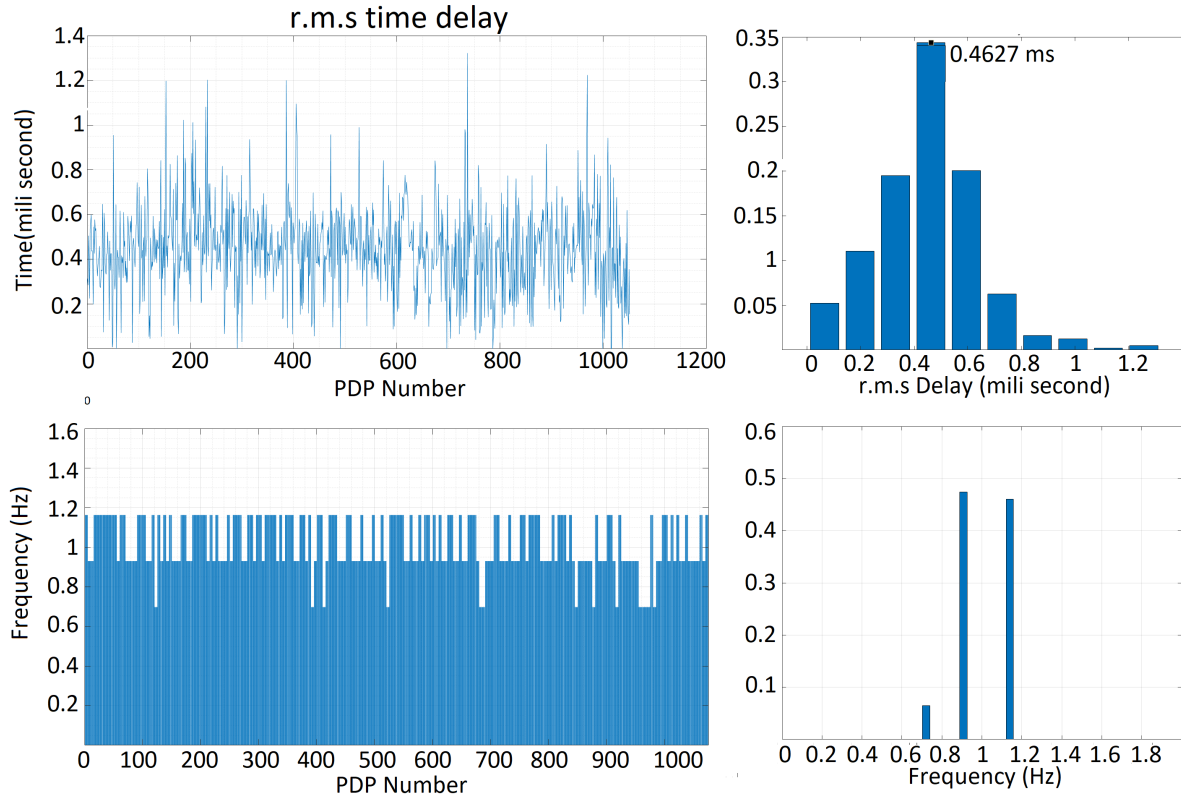


Figure 12. Result from one-day measurement for (a) Delay spread and (b) Doppler Spread

446 ms with recommendation values of Delay Spread ITU for low-latitude regions with nor-
 447 mal ionosphere conditions. This difference value is affecting the determination of dig-
 448 ital communication system parameters such as symbol period for an optimization. There-
 449 fore to have more accurate and detail values of Delay Spread, the measurement should
 450 be done for longer period. During the period of CIR measurement, ionosphere is in quiet
 451 condition based on the Kp and Dst index values which are between 0.6 to 3,6 (Matzka,
 452 2022) and -12 to -31 (World Data Center et al., 2022), respectively.

453 Figure 12b shows the variation of Doppler spread with a range from 0.7 Hz to 1.1
 454 Hz. The distribution of Doppler spread show the mean values is 0.9 Hz. Based on the
 455 Doppler spread that given by ITU, this value is higher 0.4 Hz from normal condition and
 456 lower 0.6 Hz for moderate condition in the low latitude region. This difference proba-
 457 bly occurred due to the different mechanism of ionosphere formation in the EIA region
 458 from other low latitude region. The local ionosphere tilt in equator region could affect-
 459 ing the propagation of HF radio wave path as reported in (Maruyama et al, 2006). For
 460 validation, this value could be use to calculated the apparent velocity of ionosphere move-
 461 ment as the reflection object using equation $v = \frac{f_D}{f_c} c$ where f_D is the Doppler frequency
 462 and f_c is the sounding frequency. From equation (11) with f_D is 0.9 Hz and f_c is 7.12
 463 MHz, the apparent velocity of ionosphere movement is 37,9 m/s. This value agreed with
 464 the result of vertical drift velocity of F layer ionosphere in equatorial region that done
 465 by (Namboothiri et al., 1989) which resulting the values between 10 ms to 40 ms. From
 466 early measurement result, it can be seen that the Ionosphere CIR measurement system
 467 is able to obtain the characteristic of the ionosphere channel in the form of Delay spread
 468 and Doppler spread parameters values. As the ionosphere follows the 11 years Solar cycle
 469 as the longest temporal variation, the future result from long period of mea-

470 surement could be use for comprehensive ionosphere communication channel character-
 471 istic.

472 5 Conclusion

473 The development of a channel impulse response measurement system over Java is-
 474 land, Indonesia for characterizing the Ionospheric communication channel in part of the
 475 Low latitude-Equatorial Ionosphere Anomaly (EIA) region was reported. The system
 476 resulting empirical data of Delay Spread and Doppler Spread parameter that could be
 477 used in designing the High-Frequency digital communication system. The specification
 478 of the measurement system was based on the increased value of ITU ionospheric chan-
 479 nel recommendation in order to be able to capture the possibility of higher values that
 480 occurred in the EIA regions. From the early operating testing result, slightly different
 481 values of Delay Spread and Doppler Spread from ITU were found which probably due
 482 to the effect of EIA region. This measurement system is ready to be used for collecting
 483 more data in order to characterizing the Ionosphere communication channel over Java
 484 island Indonesia in comprehensively and also for investigation and dissemination of the
 485 space weather impact on the HF communication system.

486 Open Research Section

487 All data that used in this research are belongs to National Research and Innova-
 488 tion Agency and already stored in <https://zenodo.org/record/7552900> and <https://zenodo.org/record/7619093> with title Ionospheric Channel Impulse Response Mea-
 489 surement between Pameungpeuk and Bandung, Indonesia
 490

491 Acknowledgments

492 We thanks to Dr. Rezy Pradipta from Boston College as a mentor in preparing the manuscript.
 493 We also thanks to technical team from Pameungpeuk and Bandung site for maintain-
 494 ing the operational of measurement system and for all technical support during campaign
 495 periods.

496 References

- 497 Abadi, P., Otsuka, Y., and Tsugawa, T. (2015), Effects of pre-reversal enhancement
 498 of *EB* drift on the latitudinal extension of plasma bubble in Southeast Asia,
 499 *Earth, Planets and Space*, 67–74. <https://doi.org/10.1186/s40623-015-0246-7>.
- 500 Abdu, M.A.,(2001), Outstanding problems in the equatorial iono-
 501 sphere–thermosphere electrodynamics relevant to Spread-F, *Journal of Atmo-*
 502 *spheric and Solar-Terrestrial Physics*, Volume 63, Issue 9, 2001, PP: 869-884,
 503 ISSN 1364-6826, [https://doi.org/10.1016/S1364-6826\(00\)00201-7](https://doi.org/10.1016/S1364-6826(00)00201-7).
- 504 Abdullah, S., Arief, A., and Muhammad, M., (2018). Utilization of NVIS HF Radio
 505 As Alternative Technologies In Rural Area of North Maluku. *Proceedings of*
 506 *the International Conference on Science and Technology, ICST*, pp. 734–39.
 507 doi: 10.2991/icst-18.2018.149.
- 508 Ads, A. G., P. Bergadà, J. R. Regué, R. M. Alsina-Pagès, J. L. Pijoan, D. Altadill,
 509 D. Badia, and S. Graells. (2015), Vertical and Oblique Ionospheric Sound-
 510 ings over the Long Haul HF Link between Antarctica and Spain, *Radio Sci-*
 511 *ence*,50(9):916–30. doi: 10.1002/2015RS005773.
- 512 Andersen, J. B., Rappaport, T. S., and Yoshida, S., (1995) Propagation measure-
 513 ments and models for wireless communications channels, *IEEE Communica-*
 514 *tions Magazine*, vol. 33, no. 1, pp. 42-49, Jan. 1995, doi: 10.1109/35.339880.
- 515 Angling, J., Matthew, S., Paul Cannon, C., Nigel Davies, J. Tricia Willink, Vi-
 516 vianne Jodalen, and Bengt Lundborg. (1998), Measurements of Doppler and

- 517 Multipath Spread on Oblique High-Latitude HF Paths and Their Use in Char-
 518 acterizing Data Modem Performance. *Radio Science*, 33(1):97–107.
- 519 Bergada, P., J. L. Pijoan, M. Salvador, J. R. Regué, D. Badia, and S. Graells.
 520 (2014), Digital Transmission Techniques for a Long Haul HF Link: DSSS
 521 versus OFDM, *Radio Science*, 518–30. doi: 10.1002/2013RS005203.1.
- 522 Bole, A., Wall, A., and Norris A, (2014), Chapter 2 - The Radar System – Tech-
 523 nical Principles, Radar and ARPA Manual (Third Edition), (Butterworth-
 524 Heinemann, PP: 29-137, ISBN 9780080977522, [https://doi.org/10.1016/B978-
 525 0-08-097752-2.00002-7](https://doi.org/10.1016/B978-0-08-097752-2.00002-7).
- 526 Chen, G., Zhao, Z., Zhu, G., Huang, Y., and Li, T., (2010), HF Radio-Frequency
 527 Interference Mitigation, (*IEEE Geoscience and Remote Sensing Letters*, Vol. 7,
 528 no. 3, pp. 479-482, July 2010, doi: 10.1109/LGRS.2009.2039340.
- 529 Commonwealth of Australia, Bureau of Meteorology, (2023), *ASAPS*. Retrieved
 530 from: <https://www.sws.bom.gov.au/ProductsandServices/1/2>
- 531 Cox, Donald C. (1972) , Delay Doppler Characteristics of Multipath Propagation
 532 at 910 Mhz in a Suburban Mobile Radio Environment, *IEEE Transactions on*
 533 *Antennas and Propagation* 20(5):625–35. doi: 10.1109/TAP.1972.1140277.
- 534 Davies, K. (1965), Ionospheric radio propagation (Vol. 80). *US Department of Com-*
 535 *merce, National Bureau of Standards*.
- 536 Drongowski (2020): *Ham It Up Upconverter*. Retrieve from:
 537 [https://support.noelec.com/hc/en-us/articles/360005812474-Ham-It-Up-
 538 Upconverter](https://support.noelec.com/hc/en-us/articles/360005812474-Ham-It-Up-Upconverter).
- 539 Duncan, R., A. (1960), The equatorial F-region of the ionosphere, *Journal of At-*
 540 *mospheric and Terrestrial Physics*, Volume 18, Issues 2–3, 89-100, ISSN 0021-
 541 9169, [https://doi.org/10.1016/0021-9169\(60\)90081-7](https://doi.org/10.1016/0021-9169(60)90081-7).
- 542 Eliardsson, P., Axell, E., Stenumgaard, P., Wiklundh, K., Johansson, B., and B.
 543 Asp (2015), Military HF communications considering unintentional platform-
 544 generated electromagnetic interference, *Proceeding 2015 International Confer-*
 545 *ence on Military Communications and Information Systems (ICMCIS)*, 1-6,
 546 doi: 10.1109/ICMCIS.2015.7158700.
- 547 Goodman (2005). The Ionosphere. In: Space Weather Telecommunications. *The*
 548 *International Series in Engineering and Computer Science*, vol 782. Springer,
 549 Boston, MA. <https://doi.org/10.1007/0-387-23671-63>
- 550 Goldsmith, A (2005), Wireless Communications, *Cambridge University Press* p. 86,
 551 ISBN 978-0-521-83716-3
- 552 Great Scott Gadgets (2021), *FAQ: What is the Transmit Power of HackRF?*. Re-
 553 trieved from <https://hackrf.readthedocs.io/en/latest/faq.html>
- 554 HB9JAG, (2013), *Some Measurements on DVB-T Dongles with E4000 and*
 555 *R820T Tuners: Image Rejection, Internal Signals, Sensitivity, Overload,*
 556 *1dB Compression, Intermodulation,*. Retrieved from [https://www.rtl-
 557 sdr.com/measurements-on-rtl-sdr-e4000-and-r820t-dvb-t-dongles-image-
 558 rejection-internal-signals-sensitivity-overload-1db-compression-intermodulation/](https://www.rtl-sdr.com/measurements-on-rtl-sdr-e4000-and-r820t-dvb-t-dongles-image-rejection-internal-signals-sensitivity-overload-1db-compression-intermodulation/)
- 559 Helmholtz Centre Potsdam German Research Centre for Geosciences GFZ (2023)
 560 (Kp-Index. Retrieved from: <https://kp.gfz-potsdam.de/en/data>
- 561 Icom Inc.,(2015), *ICOM IC-718 Instruction Book*. Retrieved from
 562 <https://www.icomjapan.com/support/manual/1427/>
- 563 International Telecommunication Union (2000), *Recommendation ITU-R Rec.*
 564 *F.1487. Testing of HF modems with bandwidths of up to about 12 kHz using*
 565 *ionospheric channel simulators*. Retrieved from [https://www.itu.int/rec/R-
 566 REC-F.1487-0-200005-I/en](https://www.itu.int/rec/R-REC-F.1487-0-200005-I/en)
- 567 Jiyo, (2013)., Analysis of Radio Wave Propagation Over Pameungpeuk-Bandung
 568 District Communication Circuit and Its Relations With Condition of Iono-
 569 sphere, *Jurnal Sains Dirgantara*, Vol. 11, no. 1, pp. 29-40.
- 570 Kitano, T.,Tomioka, Y., Subekti, A., Sadiq, M. A., Juzoji, H., and Nakajima,
 571 I.,(2006), A basic study of the near vertical inclined skywave the last sur-

- vival tool of radio communications to support telemedicine after n-disaster, *HEALTHCOM 2006 8th International Conference on e-Health Networking, Applications and Services*, pp. 165-169, doi: 10.1109/HEALTH.2006.246440
- Kurniawati, I, Hendranto, G., and Taufik M, (2018) Statistical Modeling of Low-Latitude Long-Distance HF Ionospheric Multi-Mode Channels. *Progress in Electromagnetic Research Vol. 64*, PP:77–86. doi: doi:10.2528/PIERM17101603.
- Laufer, C., (2014), *The Hobbyist’s Guide to the RTL-SDR: Really Cheap Software Defined Radio: Kindle Edition*. RTL-SDR.com
- Maruyama, T. and Kawamura, M.(2006), Equatorial ionospheric disturbance observed through a transequatorial HF propagation experiment, *Ann. Geophys.*, 24, 1401–1409, <https://doi.org/10.5194/angeo-24-1401-2006>.
- Maslin, N.M. (1988), *HF Communications: A Systems Approach (1st ed.)*. CRC Press., <https://doi.org/10.4324/9780203168899>
- Matzka, Jürgen; Bronkalla, Oliver; Tornow, Katrin; Elger, Kirsten; Stolle, Claudia (2021): *Geomagnetic Kp index. V. 1.0*. GFZ Data Services. <https://doi.org/10.5880/Kp.0001>
- McNamara, L., F., (1991), *The Ionosphere: Communications, Surveillance, and Direction Finding*, *Kruger Pub. Co.*, Malabar, 1991.
- Murugan, M., Purandare R., G., and Tavildar A., S., (2008), Near Vertical Incidence Skywave (NVIS) Propagation. *Proceedings of the international conference on sensors, signal processing, communication, control and instrumentation (SSPCCIN) January 3-5, VIT Pune, India*
- Munro, G. H. (1953). Reflexions from irregularities in the ionosphere. *Proceedings of the Royal Society of London A*, 219, 447–463.
- Munro, G. H., Heisler, L. H. (1958). Ionospheric records of solar eclipses. *Journal of Atmospheric and Solar-Terrestrial Physics*, 12, 57–67.
- Namboothiri, S. P., Balan, N., and Rao, P. B. (1989), Vertical plasma drifts in the F region at the magnetic equator, *J. Geophys. Res.*, 94(A9), 12055– 12060, doi:10.1029/JA094iA09p12055.
- Ossmann, M., (2016), *Software defined radio with HackRF*. Retrieved from: <https://greatscottgadgets.com/sdr>
- Pirkel, Ryan J., and Gregory D. Durgin. (2008), Optimal Sliding Correlator Channel Sounder Design, *IEEE Transactions on Wireless Communications* 7(9):3488–97. doi: 10.1109/TWC.2008.070278.
- Porte, J., Maso, J. Pijoan, J., Miret, M., Badia, D., and Jayasinghe, J., (2018) Education and e-health for developing countries using NVIS communications, *2018 IEEE Region 10 Humanitarian Technology Conference (R10-HTC)*, pp. 1-5, doi: 10.1109/R10-HTC.2018.8629842.
- Salous, S., (2013), *Radio Propagation Measurement and Channel Modelling*, 1st ed., Wiley, 2013, pp.182-191.
- Suksmono, A., B., (2013), A Simple Solution to the Uncertain Delay Problem in USRP Based SDR-Radar Systems, *arXiv* 1309.4843, pp. 1-4, 2013
- Ulversoy, T., (2010), Software Defined Radio: Challenges and Opportunities, *IEEE Communications Surveys Tutorials*, vol. 12, no. 4, pp. 531-550, Fourth Quarter 2010, doi: 10.1109/SURV.2010.032910.00019.
- Wang, J., Ding, G., and Wang, H. (2018). HF Communications: Past, Present, and Future. *China Communications*, 15, 1–9
- Withington, T. (2020, June 10). *HF Radio: Still Valid After 100 Years*. Retrieved from <https://www.asianmilitaryreview.com/2020/06/hf-radio-still-valid-after-100-years>
- World Data Center for Geomagnetism, Kyoto, M. Nose, T. Iyemori, M. Sugiura, T. Kamei (2015), *Geomagnetic Dst index*, doi:10.17593/14515-74000

1 **Channel Impulse Response Measurement for**
2 **Characterizing The Ionosphere Communication**
3 **Channel Over Java Island Indonesia**

4 **Varuliantor Dear ^{1,2}, Iskandar ¹, Prayitno Abadi³, Cahyo Purnomo⁴, Asnawi**
5 **Husin², and Adit Kurniawan¹**

6 ¹Sekolah Teknik Elektro dan Informatika - Institut Teknologi Bandung

7 ²Pusat Riset Antariksa - Badan Riset dan Inovasi Nasional

8 ³Pusat Riset Iklim dan Atmosfer - Badan Riset dan Inovasi Nasional

9 ⁴Stasiun Observasi Antariksa Atmosfer Sumedang - Badan Riset dan Inovasi Nasional

10 ¹Jl. Ganesa 20 Lebak Siliwangi, Bandung, Indonesia

11 ²Jl. Cisitua Sangkuriang, Bandung, Indonesia

12 ³Jl. Jl. Cisitua Sangkuriang, Bandung, Indonesia

13 ⁴Jl. Jl. Raya Bandung-Sumedang, Sumedang, Indonesia

14 **Key Points:**

- 15 • Development of ionosphere channel impulse response measurement system to ob-
16 tained the empirical data of Delay Spread and Doppler Spread
17 • The system is placed over Java island Indonesia which part of Low-Latitude-Equatorial
18 Ionosphere Anomaly region
19 • The system is ready to be used for collecting further data in order to character-
20 ize the ionospheric communication channel comprehensively

Corresponding author: Varuliantor Dear, varuliantor.dear@brin.go.id

Abstract

For designing a digital High Frequency (HF) radio communication system in the sky-wave propagation mode, Delay spread and Doppler spread are the fundamental parameters of ionosphere channel characteristics that need to be known. Although the International Telecommunication Union (ITU) already provides general classification values for three different regions and conditions as a recommendation, the empirical Delay spread and Doppler spread values are still needed for an optimum design. As the role of HF communication in Indonesia is still important and its development technology is continued, the empirical data of ionosphere channel characteristics are also needed. However, the comprehensive empirical data of ionosphere channel characteristics over Indonesia is difficult to find. In this research, we developed an Ionosphere Channel Impulse Response (CIR) measurement system based on Software Defined Radio (SDR) with purpose to obtain the empirical values of Delay spread and Doppler spread. The measurement system is placed in Java Island Indonesia, which is in the Low latitude - Equatorial Ionosphere Anomaly (EIA) region. The specification of the system was determined based on the increased values of ITU parameters for low-latitude regions in order to be able to capture the possibility of higher values. The early measurement result shows slightly different values from ITU recommendation which is probably due to the EIA regions effect. This system is ready to collect further data to characterize the ionospheric communication channel comprehensively and investigate the space weather impact on HF communication systems.

Plain Language Summary

Delay spread and Doppler spread are the fundamental parameter of a communication channel that should be known for designing the wireless digital communication system. Those parameters should also be known for designing the High Frequency (HF) digital communication system. Although International Telecommunication Union (ITU) already provides general values for three different locations and conditions, the empirical values of Delay spread and Doppler spread still need to be known for an optimum design. In this research, we reported the development of the ionospheric channel impulse response measurement system over Java Island Indonesia which is part of the low-latitude - Equatorial Ionosphere Anomaly (EIA) region. The purpose of the measurement system is to obtain the empirical Delay spread and Doppler Spread values with the specification of the system based on the increased values of ITU recommendation in order to be able to capture the possibility of higher values that could be occurred in the EIA region. Early measurement results show slightly different values from ITU recommendation which is probably due to the EIA region effect. This system is ready to use for collecting more data for characterizing the ionosphere communication channel comprehensively and for investigating the space weather impact on HF communication systems

1 Introduction

Ionosphere is one of the radio wave propagation mediums provided by nature for Beyond Line of Sight (BLOS) propagation in the High Frequency (HF) radio spectrum. Based on the advantages of the BLOS propagation, which are: (i) long-distance coverage area, (ii) minimum infrastructure requirement, and (iii) relatively low cost (Maslin, 1988), HF radio communication is used widely for military communication (Eliardsson et al., 2015) (Withington, 2020), post-disaster communication (Kitano et al., 2006), and regular communication with remote areas (Porte et al., 2018) (Abdullah et al., 2018). Those advantages are the basic reasons for the continuous development of HF Radio communication systems which transform into digital communication systems (Wang et al., 2018). However, for the development of an optimum digital communication systems, the fundamental information that should be known is the channel characteristic in terms of

71 Delay Spread and Doppler Spread parameters (Andersen et al, 1995). The Delay spread
72 is the spreading of the arrival time of radio wave multipath components through a chan-
73 nel, and the Doppler Spread is the spreading of the received frequency through the chan-
74 nel. Regarding to this important consideration, the characteristic of ionosphere chan-
75 nel should also be known for the design of HF digital communication system.

76 As part of space weather components, Ionosphere known as a dispersive commu-
77 nication channel which have temporal and spatial variations (Goodman, 2005). For gen-
78 eral reference in the design and test of HF digital modems, International Telecommu-
79 nication Union (ITU) already provides the ionospheric channel characteristic parame-
80 ters values as a recommendation (ITU, 2000). ITU generally classified the ionosphere
81 channel into three different regions and conditions for Delay spread and Doppler spread
82 channel parameters. The classification of three different regions of ITU are low latitude,
83 middle latitude, and high latitude. Meanwhile, the classification of three conditions of
84 the ionosphere are quiet, moderate, and disturbed. Those recommendation values are
85 helpful for basic digital communication design. However, some research shows that the
86 empirical data of channel characteristics are still needed in order to achieve the optimum
87 design for real world implementation (Ads et al., 2015) (Bergada et al., 2014) (Angling
88 et al., 1998). Therefore, for the development of HF digital communication in Indonesia,
89 the empirical data should also available. From the perspective of ionospheric physic mech-
90 anism, Indonesia is part of low latitude regions with some islands are rely on the Equa-
91 torial Ionospheric Anomaly (EIA) region. The Ionosphere in EIA regions known to have
92 higher electron density from other low-latitude regions due to the "fountain effect" mech-
93 anism (Duncan, 1960) and also a concentration of ionosphere scintillation. Therefore,
94 empirical data of ionosphere channel characteristics over Indonesia will also contribute
95 to the knowledge of the ionosphere behaviours in the low latitude-EIA regions as part
96 of space weather dissemination.

97 The Delay Spread and Doppler Spread could be obtained from the Channel Im-
98 pulse Response (CIR) measurement (Salous, 2013). To the best of our knowledge, the
99 research for measuring the channel impulse response in Indonesia is difficult to found,
100 except that has been done by Kurniawati et al.(2018). They investigated the statisti-
101 cal channel model of the ionosphere for 3044 km link between Surabaya and Merauke
102 from 5 days of measurement. Their research shows the distribution of Delay spread with
103 mean values in the range of 0–100 ms, 100–500 ms, and 500–1300 ms for 3 cluster multi-
104 hop modes namely 2F, 3F, and 4F. Those values are significantly higher compared to
105 the ITU recommendation. From our perspective, those higher values probably are not
106 defining the "pure" of ionosphere communication channel characteristics due to the fac-
107 tor of earth-surface reflections in the long haul multi-hop propagation mode. Therefore,
108 these results could not be suitable to be used for characterizing the basic ionosphere chan-
109 nel behaviours. Besides the possibility of influencing factors from the earth's surface re-
110 flection, the relative-short period of measurement are not enough to be use for three clas-
111 sification ionosphere conditions as given by ITU. For characterizing the ionosphere chan-
112 nel, this research could be improved by using different geometry of transmitter and re-
113 ceiver location alongside with its period of measurement. In this research, we develop
114 the ionosphere channel impulse response measurement system for low latitude region and
115 in Near Vertical Incidence Skywave (NVIS) propagation mode in order to obtain the em-
116 pirical Delay Spread and Doppler spread values for characterizing the ionosphere com-
117 munication channel. The development of the system is based on the Software Defined
118 Radio (SDR) platform and placed in Java island Indonesia which is rely on the crest re-
119 gion of Low Latitude-Equatorial Ionosphere Anomaly (EIA). To have a comprehensive
120 report, the structure of this paper is written as follows: in section 2 brief theory of chan-
121 nel impulse response measurement is described. In section 3, the design of the measure-
122 ment method and the determination of system parameters including the data post-processing
123 is described. In section 4 Result from operational testing and its discussion are described.
124 In the last section, the conclusion of this paper are given.

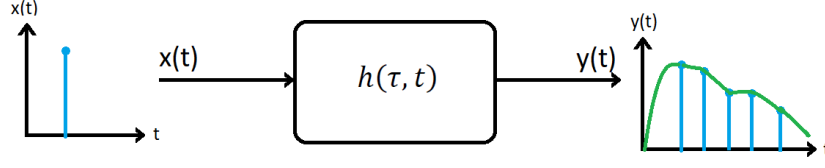


Figure 1. Linear time variant system model as representation of multipath channel.

125 **2 Channel Impulse Response Measurement**

126 A multipath wireless channel could be represented as the Linear Time-Variant model
 127 and could be characterized by its Channel Impulse Response (CIR) as illustrated in Fig-
 128 ure 1. The output of model $y(t)$ is the convolution of input $x(t)$ with the channel im-
 129 pulse response $h(t, \tau)$. From the channel impulse response, the information of multipath
 130 of radio wave propagations in the channel could be known in terms of its arrival time
 131 and its phase. For the ionosphere, the channel impulse response measurement could also
 132 be used for characterizations which needed in the design of digital communication sys-
 133 tem. The channel impulse response in the discrete form could be written as follows:

$$h(t, \tau) = \sum_{n=1}^N \alpha_n(t) e^{-j\varphi_n(t)} \delta(\tau - \tau_n(t)) \quad (1)$$

134 where α_n is the path loss and shadowing function, φ_n as the phase and Doppler func-
 135 tion, and δ is diract function for N number of multipath components. From $h(t, \tau)$, the
 136 scattering function $S(f, \tau)$ of a channel could be calculated using equation as follows:

$$S(f, \tau) = \int_{-\infty}^{\infty} R_{hh}(\Delta t, \tau) e^{-j2\phi f \Delta t} \partial \Delta t \quad (2)$$

138 where R_{hh} is the autocorrelation function of $h(t, \tau)$. The Scattering function $S(f, \tau)$ con-
 139 sists of two variable channels which are Power Delay Profile (PDP) and Doppler Spec-
 140 trum. Power Delay Profile is a function of time that describe the spreading of the time
 141 delay of the channel and could be expressed in equation as follows:

$$P(\tau) = \int_{-\infty}^{\infty} S(f, \tau) \partial f \quad (3)$$

142 For the spreading of frequency or Doppler spectrum, the calculation could done using
 143 equation as follows:

$$P(f) = \int_{-\infty}^{\infty} S(f, \tau) \partial \tau \quad (4)$$

144 From the spreading of the time delay or Delay spread and the spreading of Doppler fre-
 145 quency or Doppler spread, the Bandwidth coherence and the Time coherence of chan-
 146 nel could be obtained, respectively (Goldsmith, 2005). Bandwidth coherence and Time
 147 coherence are useful for determining the digital communication system parameters for
 148 an optimization.

149 **3 Methodology**

150 **3.1 System Design**

151 One of the popular techniques to measure the channel impulse response is a cor-
 152 relator channel sounder where firstly introduced by (Cox, 1975). In correlator channel
 153 sounder, an impulse signal which is represented by the Pseudo Random Bit Sequence

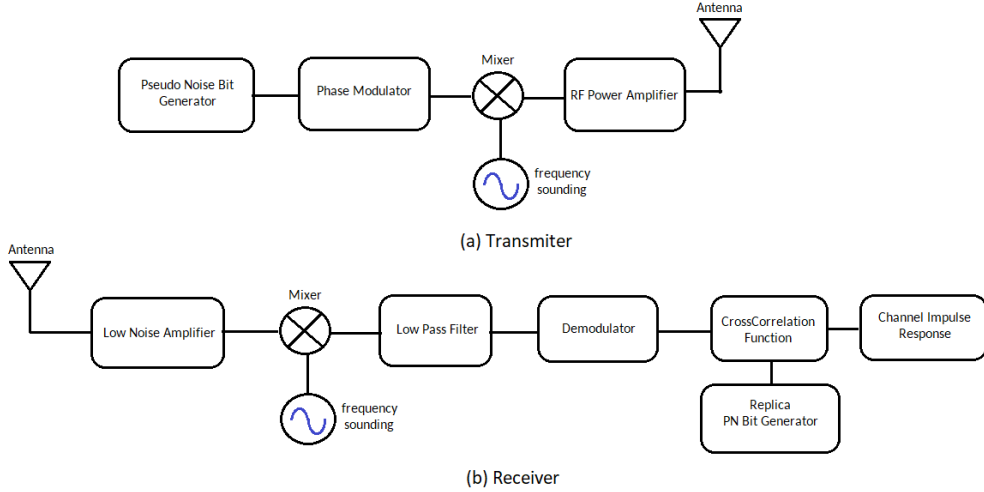


Figure 2. Correlator channel sounder block diagram for measuring the Ionospheric Channel Impulse Response.

154 (PRBS) is sent to the measured channel in order to be analyzed using its autocorrelation
 155 function on the receiver side. From the autocorrelation result, the number of gener-
 156 ated impulses in the channel could be obtained which represents the number of mul-
 157 tipath propagations in the channel. To avoid the mistaken calculation, the PRBS should
 158 have a good autocorrelation property. There are some PRBS that could be selected such
 159 as Maximum Length Sequence, Barker code, Gold code, and Kasami code (Salous, 2013).
 160

161 The block diagram of the correlator channel sounder for measuring the Ionosphere
 162 channel impulse response is shown in Figure 2. The transmitter block consists of Pseudo
 163 Noise (PN) code generator, Phase Modulator, Mixer, Radio Frequency Power Amplifier
 164 (RFPA), and Antenna. The PN code generator block generates the Pseudo Random Bit
 165 Sequence. In this study, the Maximum Length Sequence (MLS) bit was chosen. The PN
 166 bit sequence is then phase-modulated by the phase modulator block. The signal from
 167 the output of the modulator block is shifted from baseband frequency to the selected pass-
 168 band frequency in the mixer block. The magnitude of the signal output from the mixer
 169 block is increased in the RFPA block before being transmitted to the air by the antenna.

170 On the receiver side, the block diagram consists of Antenna, Low Noise Amplifier
 171 (LNA), Mixer, Low Pass Filter (LPF), Demodulator, and Cross-Correlation function to-
 172 gether with replica of the transmitted PN Bit Generator as part of the signal process-
 173 ing block. The magnitude of the received signal from the antenna is increased in the LNA
 174 block and then down-shifted to the baseband frequency by Mixer and Low Pass Filter
 175 block. The signal output from the Low Pass Filter block is then demodulated in the De-
 176 modulator block and continued to be processed in the cross-correlation function block
 177 using the replica of the transmitter PN bit sequences. The output of cross correlation
 178 function block is the channel impulse response which used to analyze the ionosphere chan-
 179 nel characteristics.

180 3.2 Determination of Software Defined Radio Parameters

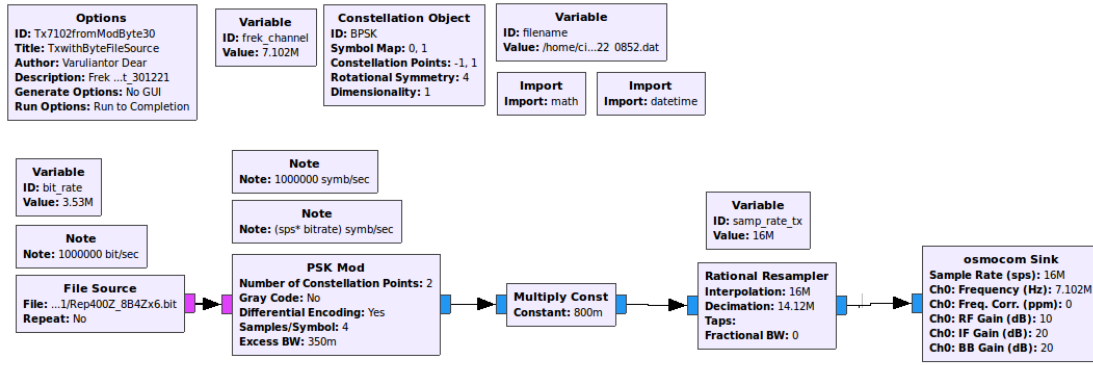
181 The temporal and spatial variation of the ionosphere are needed to be considered
 182 when determining the specification of the Ionosphere CIR measurement system. For mea-

183 suring the ionosphere channel characteristic over Java Island, Indonesia, the basic spec-
 184 ification of CIR measurement system could be chosen from ITU recommendation doc-
 185 ument for low latitude region as the minimum values. Those values are increased with
 186 the consideration that Java Island is part of the crest region of Equatorial Ionosphere
 187 Anomaly (EIA), which probably have higher values. The specification parameters of the
 188 ionosphere CIR measurement system are Time delay resolution (τ_{res}), Delay maximum
 189 (τ_{max}), and Maximum Doppler Frequency (fD_{max}). For this ionosphere CIR measure-
 190 ment system, the resolution of time delay is selected to be 5 times higher than the de-
 191 lay spread values from ITU recommendation for low latitude region in normal condition.
 192 The selected value was based on the consideration of the possibility of faster arrival time
 193 between each propagation path in the ionosphere. For the maximum of the time delay,
 194 the selected value is also 5 times higher than ITU Delay spread recommendation for low-
 195 latitude region with disturbed condition. The consideration of these selected values was
 196 from the possibility of the larger number of multi-hop radio wave propagation due to the
 197 occurrence of Equatorial Spread-F (ESF) which makes the ionosphere layer is in unsta-
 198 ble conditions (Abdu, 2001). For the Doppler frequency maximum, the selected value
 199 was 2 times higher than the value of Doppler Spread that given by ITU in low latitude
 200 region with disturbed condition. The Doppler frequency value could be increased more
 201 by using the sliding correlator technique in the post processing stage (Pirkl and Durgin,
 202 2008). Those specification parameters value will determine the parameter value of cor-
 203 relator channel sounder that used for this CIR measurement system design. In Table 1,
 204 the relation between target value for specification of ionosphere CIR measurement sys-
 205 tem with the ITU recommendation values are presented.

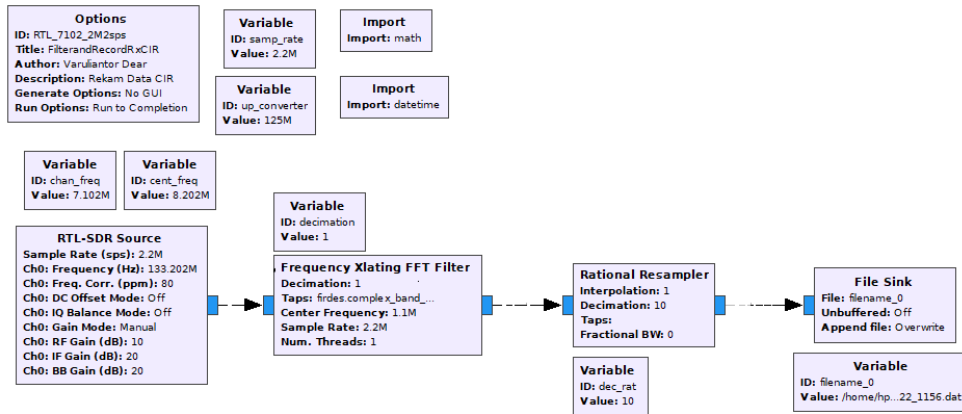
Table 1. Determination of ionosphere CIR specification target

Parameter	ITU Rec F.1487 Value	Target Value	Remark
Time delay resolution (τ_{res})	0.5 ms	0.1 ms	Delay Spread for low latitude with Quiet Condition
Max time delay (τ_{max})	6 ms	30 ms	Delay Spread for low latitude with Disturb Condition
Max Doppler frequency (fD_{max})	10 Hz	>10 Hz	Doppler Spread for low latitude with Disturb Condition

206 For optimum practical implementation, the determination of channel sounder pa-
 207 rameter values could use algorithm that provided by (Pirkl and Durgin, 2008). In this
 208 observation system, we determine the SDR parameters that will be used for the contin-
 209 uous operational system. The GNU Radio block diagram that used for implementing the
 210 correlator channel sounder is shown in Figure 3. In the transmitter side, file source block
 211 is used to read the prepared file which consists of PN bit sequence. The PN bit sequence
 212 from file source block are modulated by the Phase Shift Key (PSK) modulation block
 213 and resulting the modulated signal in the baseband spectrum. This modulated signal
 214 is re-sampled in the block rational resampler to meet the required sampling rate of Os-
 215 smocom sink block that used for shifting the signal to the selected sounding frequency
 216 while maintaining the bit rate. The Osmocom sink block is related with the specifica-
 217 tion of SDR hardware that used for transmitting the signal over the air. In this study
 218 HackRF one is used for the transmitter SDR hardware with sampling rate up to 20 Mega
 219 Symbols per Second (MSps) and frequency range 100 kHz to 6 GHz (Ossmann, 2016).
 220 From the configuration block diagram in GNU Radio and using an assumption that for



(a) Transmitter



(b) Receiver

Figure 3. Implementation of Correlator Channel Sounder in the GNU Radio software

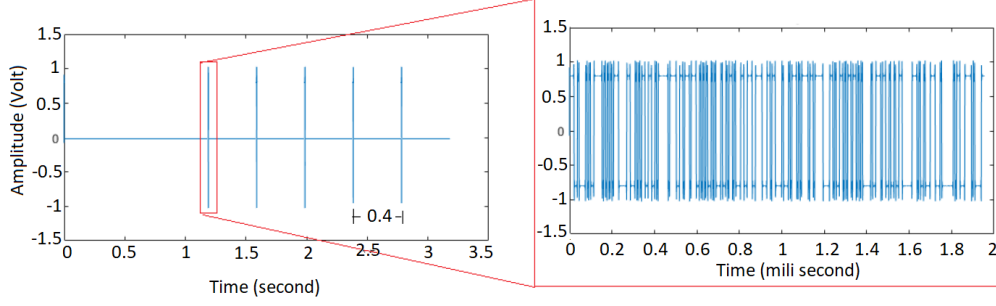


Figure 4. Waveform of sounding signal

221 one transmission is only consists of a single chip waveform, the determination of sam-
 222 pling rate values to meet the specification target in Table 1 could be use equation $Samplingrate =$
 223 $sps.bitrate$ where sps is the number of sample per symbol in modulator block diagram
 224 and bit rate is the number of bit that should be transmitted in one second which is equal
 225 to f_{chip} value. The modulation that use is Binary Phase Shift Keying (BPSK). There-
 226 fore, the values of sps is 2 which resulting the minimum of sampling rate is 20000 sam-
 227 ple per symbol. This value is below the specification of the SDR hardware and poten-
 228 tially could be implemented. Regarding to the target of time delay maximum and chip
 229 rate value, the bit PN sequence length could be determined using equation as follows:

$$230 \quad L = \tau_{max} f_{chip} = \frac{\tau_{max}}{\tau_{res}} \quad (5)$$

231 which resulting the length of PN bit sequence is 300. However, as the generation of Max-
 232 imum Length Sequence bit is in the form of shift register where the length value is based
 233 on powers of 2, the closest value is 255 which resulted from 2^8 . This selection of L will
 234 result τ_{max} is 25.5 ms. Although this value is different from the targeted delay maximum
 235 specification value, this value still higher compared to the ITU recommendation and could
 236 be accepted for the design of the ionosphere CIR measurement system.

237 The use of bit PN sequence with length 255 as the waveform for single sounding
 238 signal is already met with the specification target of CIR System. However, based on the
 239 consideration to the many possibilities of interference in the HF spectrum (Chen et al.,
 240 2010), the modification of sounding signal should be done with purpose to anticipate the
 241 interferences. Therefore, the sounding signal were modified by reshaping the waveform
 242 into 5 cluster of PN bit sequence with different time from each nearest neighbour of clus-
 243 ter PN bit is set to 0.4 second as shown in Figure 4. Beside for the redundancy purpose,
 244 the modification also intended for easier detection in the receiver side as the waveform
 245 contains more energy (Bole et al., 2014). This signal sounding modification is not chang-
 246 ing the chip rate value of the system.

247 For the implementation of the receiver block in the GNU Radio, the block diagram
 248 is simpler than the transmitter as it is intended for the post-processing technique. The
 249 block diagram are consist of RTL-SDR, Frequency Xlating FFT Filter, Rational Resam-
 250 pler, and File Sink Block. RTL-SDR and Frequency Xlating FFT Filter block are used
 251 for capture the passband signal and shifted to the baseband forms. The baseband sig-
 252 nal then resampler using rational resampler block to reduce the bandwidth of received
 253 signal up to 220 kHz which inherently reduced the size of the received signal without los-
 254 ing any information that needed for CIR calculation. At the File Sink block, the received
 255 signal were recorded for post-processing stage. The parameters of RTL SDR Block are
 256 related to the parameter of SDR hardware device which are sampling rate and frequency.
 257 In this study, the RTL-SDR hardware with chipset RTL2832U is used. The frequency

258 range and sampling rate maximum of RTL-SDR hardware is 50 MHz to 1,8 GHz and
 259 3,2 Msps, respectively (Laufer, 2014). Based on RTL-SDR device specification, the RTL-SDR
 260 could not capture the signal in the High Frequency spectrum. Therefore, the RTL SDR
 261 should be companion with Ham-It-Up Converter device which have function for direct
 262 sampling process. The combination with Ham-It-Up make RTL-SDR hardware able to
 263 capture the signal below 30 MHz (Drongowski, 2020). With this configuration, the value
 264 of frequency in the RTL-SDR block should also modified by adding the selected of sound-
 265 ing frequency with 125 MHz. The parameter values of GNU radio and its relation to achieved
 specification of CIR system are shown in Table 2.

Table 2. GNU Radio parameter values and achieved specification of CIR measurement system

Parameter	Value
f_{chip}	10000 bps
L_{PN}	255 bit
$Samp\ rate$	20000 symb/s
sps	2
τ_{res}	0.196 ms
τ_{max}	25.5 ms
fD_{max}	19.6 Hz

266

267

3.3 Additional Consideration for System Development

268

269

270

271

272

273

274

275

276

277

278

279

280

281

3.3.1 Determination of Transmitter and Receiver Locations

282

283

284

285

286

287

288

289

290

291

292

293

The transmitter and receiver locations for the CIR measurement are Pameungpeuk West Java (7.65S, 107.69E) and Bandung West Java (6.89 S, 107.59 E), respectively. The selection of those locations was firstly based on the available location and resources for long duration and continuous measurement purpose. The HF radio wave propagation between Pameungpeuk and Bandung already analyzed by (Jiyo, 2010) which conclude that the propagation of HF radio wave is only in the skywave propagation. The considerations of transmitter and receiver locations was also based on the availability of ionosonde instrument in Pameungpeuk which could provide the ionosphere density profile for confirmation and validation of the ionosphere conditions for this research. The map of transmitter and receiver locations are shown in Figure 6. The terrain between Bandung and Pameungpeuk is an east-west mountain chains which naturally blocking the ground wave propagation mode.

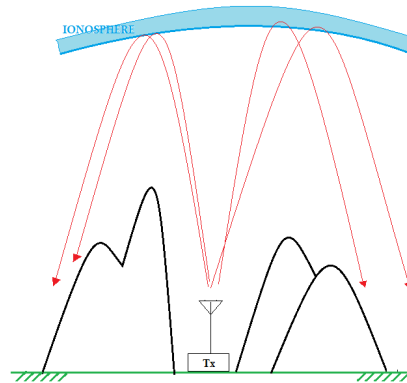


Figure 5. Illustration of Near Vertical Incident Skywave (NVIS) propagation mode

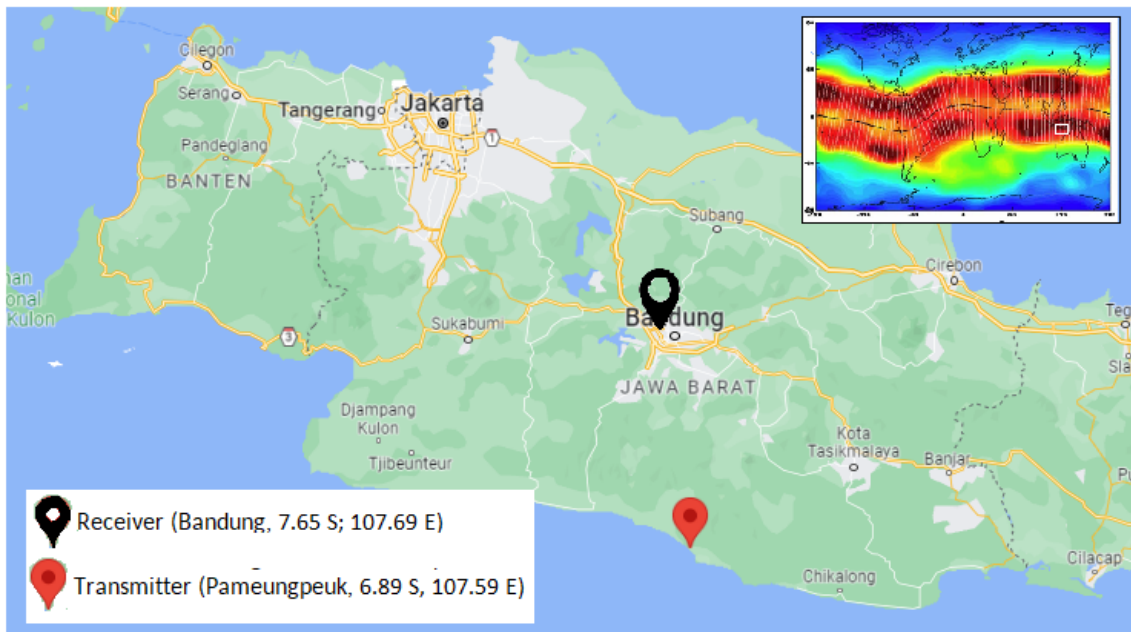


Figure 6. Location of Transmitter and Receiver Station

294

3.3.2 Selection of Sounding Frequency

295

296

297

298

299

300

301

302

303

304

305

306

307

308

309

310

311

312

313

314

The variation of ionosphere plasma density is affecting the frequency of radio wave that could be “reflected” to the earth’s surface. Therefore, to overcome this condition, the selection of the sounding frequency could be based on the frequency management method that usually use in HF radio communication plans (Maslin, 2017). In the frequency management method, the frequency was selected based on the variation of critical frequency of F layer (foF2) and minimum frequency (fmin) parameters from the ionosphere model. The frequency with the highest probability to appear between the foF2 and fmin values in the period of communication time is selected in order to guarantee the success of communication. In this study, the selection of the sounding frequency for CIR measurement is using Frequency management method based on the ionosphere model from Ionosphere Prediction System (IPS) Australia, namely Advance Stand Alone Prediction System (ASAPS) software (Commonwealth of Australia, Bureau of Meteorology, 2022). Model of foF2 and fmin were calculated for Bandung-Pameungpeuk circuits where its result shown in Figure 7. The models output from ASAPS are the Maximum Usable Frequency (MUF) and Absorption Lowest Frequency (ALF) which representing the foF2 and fmin values, respectively. From the model results, sounding frequency that selected in the CIR measurement are 3.453 MHz that used from 00:15 to 07:30 LT (UTC+7), and 7.102 MHz that used from 07:45 LT – 00:00 LT. The selection of those frequencies were also based on the legal permission to be use in the real world environment, as the author is member of amateur radio organization in Indonesia, namely ORARI.

315

3.3.3 Transmission Schedule and Measurement Timing

316

317

318

319

320

321

322

323

324

325

326

327

328

329

330

The measurement system is intended to be operated continuously and collect the result for a long period of measurement in the form of recording files. Therefore, the CIR measurement system needs to be set to work automatically and periodically for the effective and efficient of recorded file size. The CIR system is scheduled to work every 15 minutes for 24 hours a day with synchronization of sounding and recording time based on the internet reference time. However, due to the uncertainty of the time delay process from the SDR instrument (Ulversøy, 2010; Suksmono, 2013), a mismatch between the transmission and receiving time could occur. Therefore, to overcome this uncertainty of lag time, the scheduled time is added with time tolerance values both on the transmitter and receiver side. In the transmitter, the time for sounding the signal is set to start 3 seconds ahead of the recording signal in the receiver. On the receiver side, the recording time duration is extended three times from the sounding signal time duration in the transmitter. In practice, the scheduled transmission and receiving process is done using the Crontab-e functions that are already provided in UBUNTU operating system.

331

3.3.4 Link Budget Calculation

332

333

334

335

The output power of the transmission signal from HackRF one SDR device is only up to 0.03W (Great Scott Gadgets, 2021). To guarantee the transmitted signal could be arrived in the receiver antenna, the minimum required transmitted power could be calculated using equations as follows:

$$P_R = P_T + G_T + G_R + P_L \quad (6)$$

336

337

338

339

where P_R is the received Power (dBm), P_T is transmitted power (dBm), G_T is transmitted antenna gain (dBi), G_R is the received antenna gain (dBi), and P_L is the Path Loss (dB). For skywave propagation mode, P_L could be calculated using equation as follows:

$$P_L = L_a + L_{FSL} + L_g + L_p + L_q \quad (7)$$

340

341

where L_a is the absorption loss, L_g is ground loss, L_p is the polarization loss, L_q is the Loss from E layer, and L_{FSL} is the Free Space Loss. Regarding to McNamara (1991),

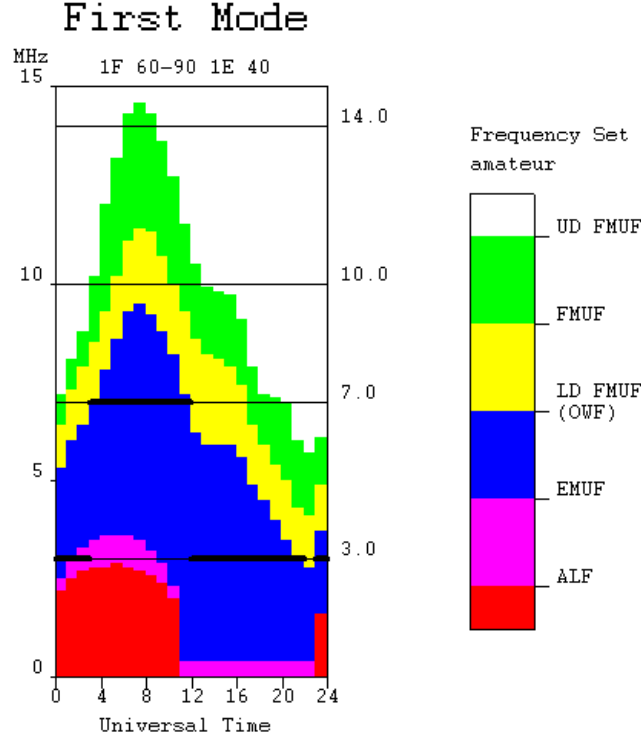


Figure 7. Result from ASAPS software for Bandung-Pameungpeuk circuits in December 2021. The selection of sounding frequency is based on the values between ALF and MUF

342 the maximum values of L_a , L_g , L_p , dan L_q is 20 dB, 3 dB, 6 dB and 9 dB, respectively.
 343 The value of L_{FSL} could be obtained using equation as follows:

$$L_{FSL} = 32,4 + 20\log(d) + 20\log(f) \quad (8)$$

344 where d is the distance of radio wave propagation path (km), and f is the frequency of
 345 radio wave (MHz). For NVIS propagation in this research, the distance (d) value is as-
 346 sumed to be 500 km and the frequency is 7 MHz. The distance value is obtained from
 347 two times values of average virtual height of F layer ($h'F$) which is 250 km. Using equa-
 348 tion (8) and (9) the Path Loss value is 103,28 dB. For the minimum of required trans-
 349 mitted power, the minimum of P_R values could be based on the RTL-SDR receiver sen-
 350 sitivity which is -139 dBm (HB9JAG, 2013)). From equation (7) the minimum required
 351 of P_T is 4.2 mW to guarantee the signal will be received in the receiver. In this CIR mea-
 352 surement system, the modul of Radio Frequency Power Amplifier (RFPA) and Low Pass
 353 Filter (LPF) from commercial HF radio transmitter Icom IC-718 are used as shown in
 354 topside of Figure 8. The average output power from this module is up to 100 Watt for
 355 Amplitude Modulation and Single Side Band transmission (Icom Inc., 2015) which enough
 356 to be used in this system although some loss from cables and connector occurred. To-
 357 gether with the use of RFPA and LPF module in the transmitter site, the HF Broad band
 358 Folded Dipole Antenna is used for an effective signal transmission over the air. At the
 359 receiver site, the similar 30 meter long wire antenna is also use but with simpler receiver
 360 hardware device as shown in bottom side of Figure 8. The specification of the hardware
 361 that used in the CIR measurement system are described in Table 3.



(a) Computer (b) HackRF One SDR (c) ICOM IC-718 (d) Power Supply (e) HF Broadband Folded Dipole Antenna

Transmitter Site



(a) RTL-SDR with Hamit-Up converter (b) Computer (c) HF Broadband Folded Dipole Antenna

Receiver Site

Figure 8. Hardware device for transmitter site (topside) and receiver site (bottom side)

Table 3. Hardware Device and Specification of Ionosphere CIR measurement system

Device	Transmitter	Receiver
SDR Hardware	HackRF One 20 Msps	RTL-SDR with HamitUp 3.2 Msps
SDR Software	GNU Radio 3.7	GNU Radio 3.7
Antenna	ICOM AH-710 (3-30 MHz)	ICOM AH-710 (3-30 MHz)
Personal Computer	Core i3 with UBUNTU 16.04	Core i3 UBUNTU 18.06
RF Power Amplifier	Icom IC-718 <i>Power</i> up to 100 Watt	none

3.4 Data Post Processing

The recorded of the received signal $r(t)$ are in the form of complex values which could be written as follows:

$$rt = s(t) * h(t) \quad (9)$$

where $s(t)$ is the transmitted signal and $h(t)$ is the ionosphere channel impulse response. To obtain the ionosphere channel impulse response from the recorded signal, the cross-correlation calculation between $r(t)$ and $s(t)$ could be done using equation as follows:

$$h(\tau) = r_{sr}(\tau) = \int_{-\infty}^{\infty} s(t)r(\tau + t)\partial\tau \quad (10)$$

where $r_{sr}(\tau)$ is the cross-correlation between $s(t)$ and $r(t)$. According to (Sakar, 2003), the obtained of ionospheric channel impulse response are representing the Power Delay Profile (PDP) that can be written in equation (1). From Power Delay Profile, the calculation of the root mean square (r.m.s) of time delay or delay spread could be done using equation as follows:

$$\tau_{rms} = \sqrt{\frac{\sum_i |\alpha|^2 (\tau_i - (\frac{\sum_i |\alpha|^2 \tau_i}{\sum_i |\alpha|^2}))^2}{\sum_i |\alpha|^2}} \quad (11)$$

where τ_i is the time delay for each path i . For the calculation of the Doppler spread, equation (8) could be use to calculate the Doppler Spectrum $S(f)$ using equation as follows:

$$S(f) = \int_{-\infty}^{\infty} r_{hh}(\Delta t, \tau) e^{-j2\phi f \Delta t} \partial \Delta \tau \quad (12)$$

where r_{hh} is the autocorrelation of ionosphere channel impulse response. From the half of Doppler spectrum values, the Doppler spread could be determined.

4 Result From Operational Testing

An example result of the recorded received signal from single measurement is shown in Figure 9. This received signal will be used in the post-processing stage to obtain the ionosphere channel impulse response and its analysis. The received signal is shown in the form of time domain and frequency domain in the Intermediate Frequency (IF) spectrum. From the time-domain graph in Figure 9, the target of the received signal that will be used for the post-processing stage could not be seen clearly. However, in the frequency domain, the targeted of the received signal could be seen clearly which appears between 1 kHz to 3 kHz and starting from the second and ending at the fifth second of the recording time. The duration of the targeted received signal is matched with the duration of transmitted sounding signal as shown in Figure 4. From the received signal in Figure 9, it can be seen also that the receiver was able to receive another signal with different frequencies. During the measurement periods, some signals with significant power,

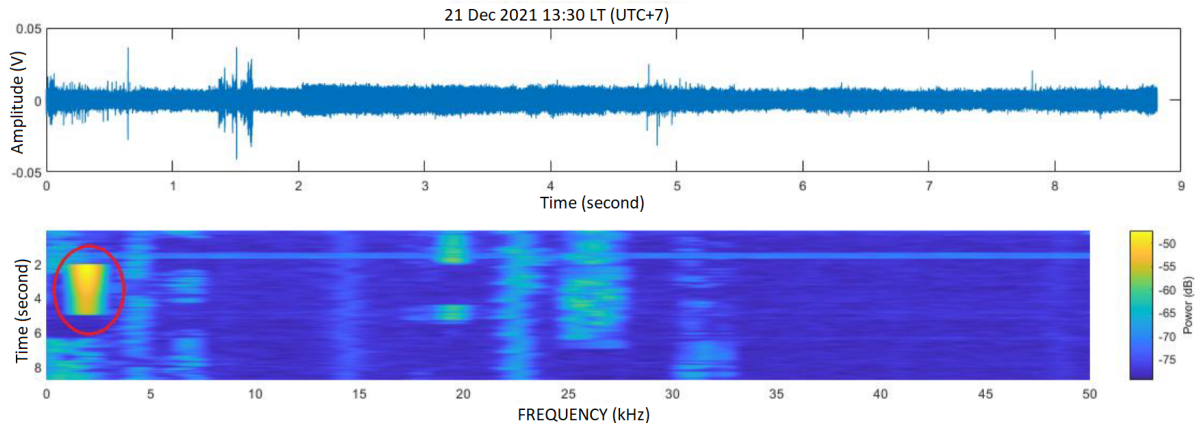


Figure 9. The received signal on 21 December 2021 at 13:30 LT (GMT+7). The targeted of the received sounding signal is between the 2nd and 5th second in the range of 1 kHz to 2.5 kHz at the Intermediate Frequency spectrum. The recorded signal also shows other received signals in different range of frequencies with significant power, bandwidth, and duration.

bandwidth, and durations in the frequencies 1 kHz, 4 kHz, 7 kHz, 15 kHz, 23 kHz, 26 kHz, and 32 kHz are also recorded. Those signals are representing another signal with different carrier frequency where its source could not be exactly identified as it could be from an amateur radio signal or broadcast station. In the range of the selected sounding frequency and in the transmission time period, it can be seen also there are some interference signals from the neighbour frequencies which could be influencing the post-processing of the received signal. From the Figure, it can be seen also that before the sounding signal was received, a wide band signal with a short period transmission time was received. This impulsive signal interference types is possible to be occurred in the same time of transmission sounding signal in the future and could not be avoided. Therefore, the redundancy technique by using 5 clusters of repeated PN bit sequences that are already explained in the methodology section is used for a mitigation.

From the received signal in Figure 9, the result of ionospheric channel impulse response calculation are shown in Figure 10. The observed of channel impulse response are consist of five cluster of Power Delay Profile with time different between the nearest neighbour cluster is around 0.4 second which follows the transmitted sounding signal as shown in Figure 4. From Figure 10b it can be seen the different number and magnitude of received impulse signal for each group. Those results show the system can captured the variation of the ionosphere channel in term of its propagation time delay. The smallest time delay that captured is 0.22 ms (CIR #1) and the highest time delay is 1.8 ms (CIR #3). Based on the specification of time delay resolution and the smallest value of delay spread given by ITU, the measurement system shows its capability to capture the ionosphere channel variation according to its specification designed. However, based on the values of the maximum of time delay that obtained in this result, the design of CIR systems could not confirm it's capabilities, yet. This condition could be occurred due to the quiet condition of ionosphere during the observation time. In Figure 11, ionogram from ionosonde during observation of CIR is shown to confirm the ionosphere conditions from its traces. It can be seen that the trace of the echo signal has clear and smooth shape without a small cusp or twist, and not spreading in time either in frequency which indicate the normal of ionosphere layers (Munro, 1953) (Munro and Heisler, 1958). From the confirmation of the quiet ionosphere condition in Figure 11, the maximum of time delay that obtained are reasonable and could be accepted.

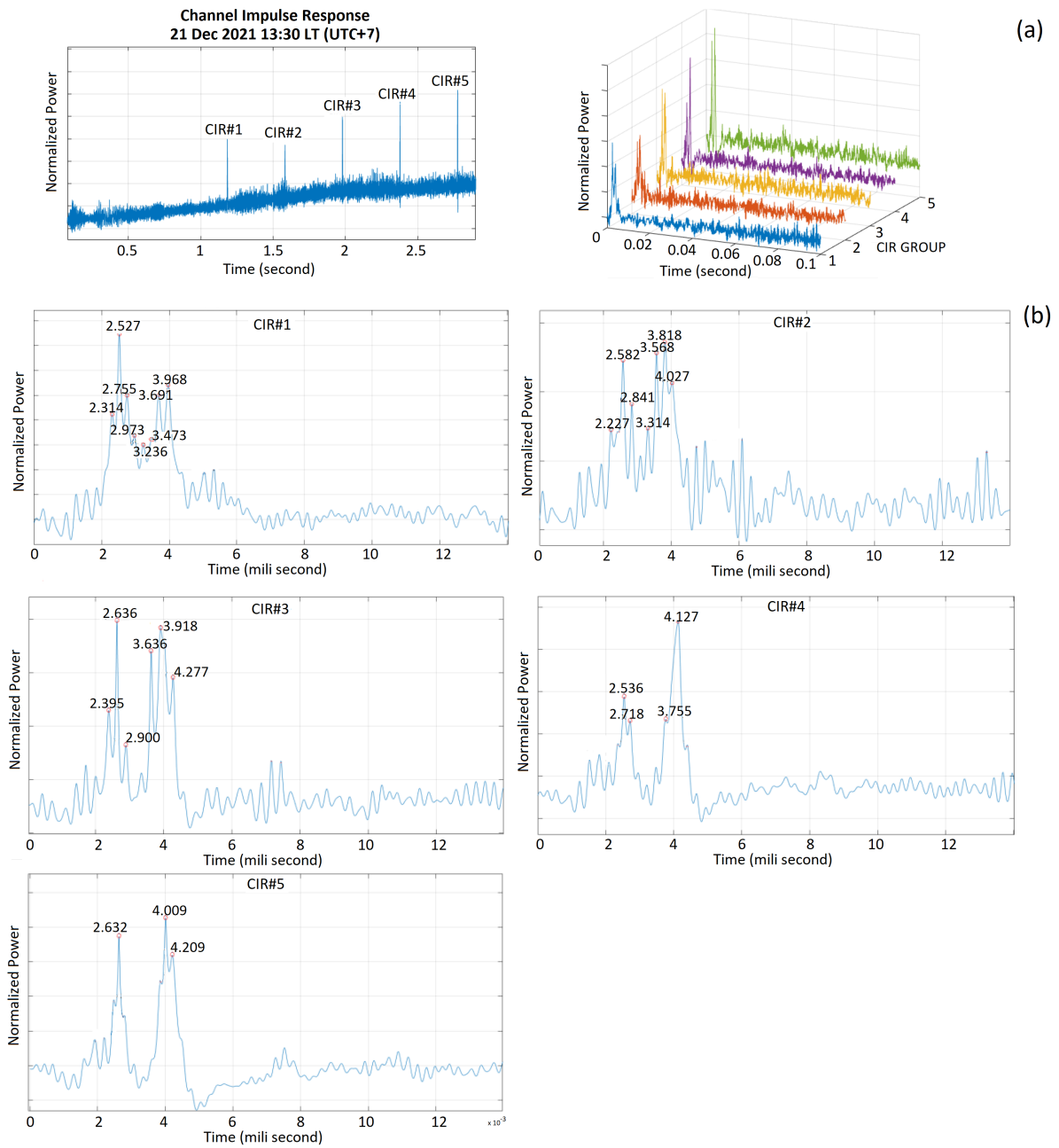


Figure 10. Ionospheric Channel Impulse Response result from 21st December 2021 at 13:30 LT (UTC+7). Five group of CIR was observed with two impulse cluster with different number and magnitude.

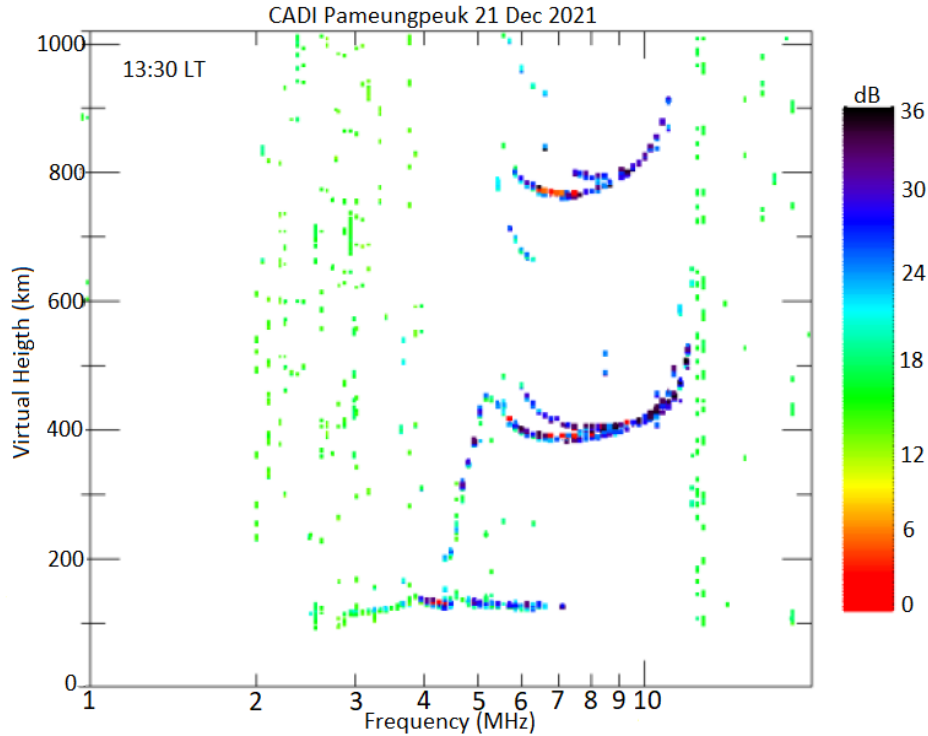


Figure 11. Ionogram from ionosonde at Pameungpeuk during the observation of CIR at 13:30 LT (UTC+7) on 21st December 2021 for the confirmation the stability and normal ionosphere conditions.

422 From ionogram in Figure 11, it can be seen also that E Sporadic layer were appeared
 423 with critical frequencies ($foEs$) values more than 7 MHz where the CIR sounding frequency
 424 is used. The impact of the existence of E Sporadic layer was captured in the 5 group of
 425 CIR measurement result. In each of CIR group, we can see two cluster of impulse with
 426 variate amplitude (Figure 10). The presences of E Sporadic layer in the received impulse
 427 could be confirmed from its apparent distance calculation compared to the distance be-
 428 tween virtual height of F layer and E layer. The different time between first impulse of
 429 second cluster and last impulse of first cluster in CIR #1 is $3.691 - 2.314 = 1.377$ ms. There-
 430 fore, the calculation of apparent distance travelling time between those two impulse clus-
 431 ters using speed of light c is 300000 km/s is 413.1 km. Half of this values is the estima-
 432 tion of different virtual height of E ($h'E$) and F ($h'F$) layers which is around 200 km. In
 433 this system, the absolute time delay that could be used for calculating the distance of
 434 the propagation path was not measured for the simplicity and the low cost of the designed
 435 system.

436 Early result measurement in the form of variation of Time Delay and Doppler frequ-
 437 ency with their distributions from 15th December 2021 to 21st December 2022 are shown
 438 in Figure 12. Figure 12a show the root mean square (r.m.s) of time delay with its dis-
 439 tribution. The r.m.s of time delay for 7 days observation is fluctuated with in range be-
 440 tween 0 to $1,3$ ms. This fluctuation show the ionosphere channel is change randomly. To
 441 obtained the general value of Delay spread, the statistical analysis approach of root mean
 442 square time delay could be done by using its distribution. From the distribution in Figure
 443 12a, it can be seen that the mean of r.m.s delay spread is 4.627 ms and follows the
 444 Rayleigh distribution with the Delay spread values are tend to have more occurrence be-
 445 low its mean values. This one-week Delay Spread measurement values is different 0.373

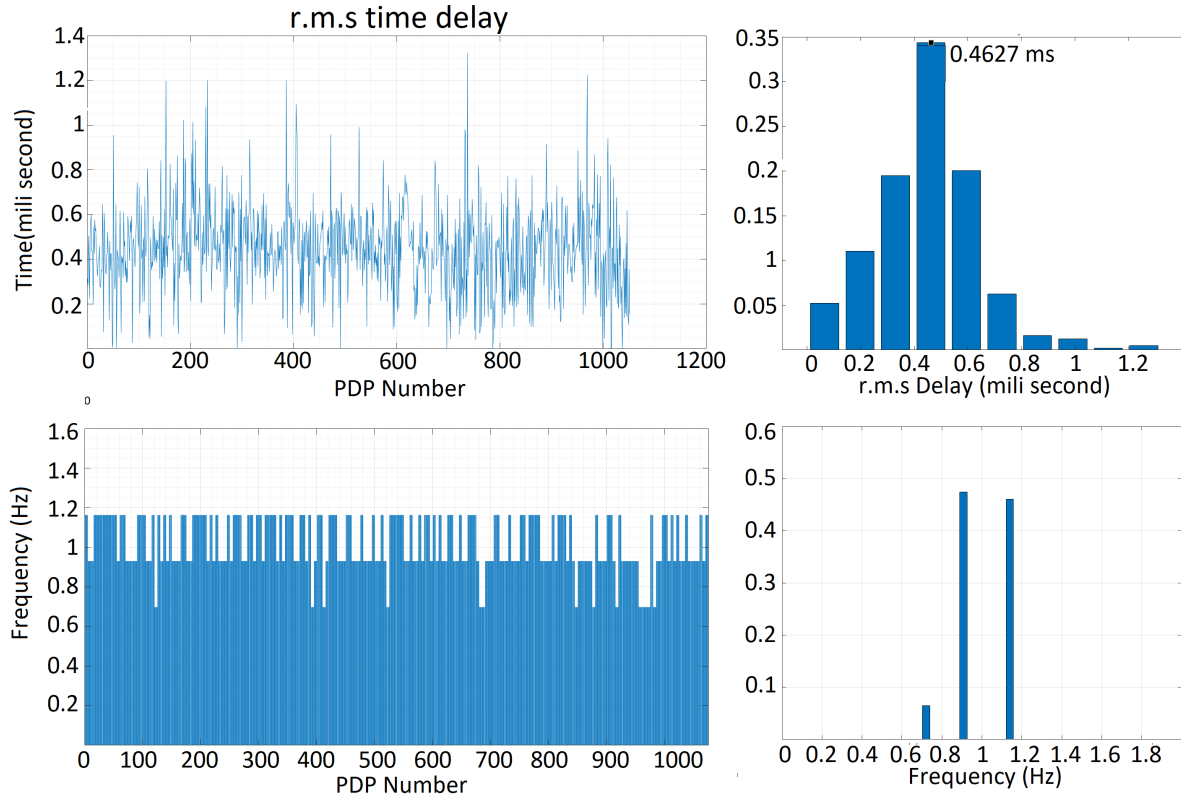


Figure 12. Result from one-day measurement for (a) Delay spread and (b) Doppler Spread

446 ms with recommendation values of Delay Spread ITU for low-latitude regions with nor-
 447 mal ionosphere conditions. This difference value is affecting the determination of dig-
 448 ital communication system parameters such as symbol period for an optimization. There-
 449 fore to have more accurate and detail values of Delay Spread, the measurement should
 450 be done for longer period. During the period of CIR measurement, ionosphere is in quiet
 451 condition based on the Kp and Dst index values which are between 0.6 to 3,6 (Matzka,
 452 2022) and -12 to -31 (World Data Center et al., 2022), respectively.

453 Figure 12b shows the variation of Doppler spread with a range from 0.7 Hz to 1.1
 454 Hz. The distribution of Doppler spread show the mean values is 0.9 Hz. Based on the
 455 Doppler spread that given by ITU, this value is higher 0.4 Hz from normal condition and
 456 lower 0.6 Hz for moderate condition in the low latitude region. This difference proba-
 457 bly occurred due to the different mechanism of ionosphere formation in the EIA region
 458 from other low latitude region. The local ionosphere tilt in equator region could affect-
 459 ing the propagation of HF radio wave path as reported in (Maruyama et al, 2006). For
 460 validation, this value could be use to calculated the apparent velocity of ionosphere move-
 461 ment as the reflection object using equation $v = \frac{f_D}{f_c} c$ where f_D is the Doppler frequency
 462 and f_c is the sounding frequency. From equation (11) with f_D is 0.9 Hz and f_c is 7.12
 463 MHz, the apparent velocity of ionosphere movement is 37,9 m/s. This value agreed with
 464 the result of vertical drift velocity of F layer ionosphere in equatorial region that done
 465 by (Namboothiri et al., 1989) which resulting the values between 10 ms to 40 ms. From
 466 early measurement result, it can be seen that the Ionosphere CIR measurement system
 467 is able to obtain the characteristic of the ionosphere channel in the form of Delay spread
 468 and Doppler spread parameters values. As the ionosphere follows the 11 years Solar cycle
 469 as the longest temporal variation, the future result from long period of mea-

470 surement could be use for comprehensive ionosphere communication channel character-
 471 istic.

472 5 Conclusion

473 The development of a channel impulse response measurement system over Java is-
 474 land, Indonesia for characterizing the Ionospheric communication channel in part of the
 475 Low latitude-Equatorial Ionosphere Anomaly (EIA) region was reported. The system
 476 resulting empirical data of Delay Spread and Doppler Spread parameter that could be
 477 used in designing the High-Frequency digital communication system. The specification
 478 of the measurement system was based on the increased value of ITU ionospheric chan-
 479 nel recommendation in order to be able to capture the possibility of higher values that
 480 occurred in the EIA regions. From the early operating testing result, slightly different
 481 values of Delay Spread and Doppler Spread from ITU were found which probably due
 482 to the effect of EIA region. This measurement system is ready to be used for collecting
 483 more data in order to characterizing the Ionosphere communication channel over Java
 484 island Indonesia in comprehensively and also for investigation and dissemination of the
 485 space weather impact on the HF communication system.

486 Open Research Section

487 All data that used in this research are belongs to National Research and Innova-
 488 tion Agency and already stored in <https://zenodo.org/record/7552900> and <https://zenodo.org/record/7619093> with title Ionospheric Channel Impulse Response Mea-
 489 surement between Pameungpeuk and Bandung, Indonesia
 490

491 Acknowledgments

492 We thanks to Dr. Rezy Pradipta from Boston College as a mentor in preparing the manuscript.
 493 We also thanks to technical team from Pameungpeuk and Bandung site for maintain-
 494 ing the operational of measurement system and for all technical support during campaign
 495 periods.

496 References

- 497 Abadi, P., Otsuka, Y., and Tsugawa, T. (2015), Effects of pre-reversal enhancement
 498 of *EB* drift on the latitudinal extension of plasma bubble in Southeast Asia,
 499 *Earth, Planets and Space*, 67–74. <https://doi.org/10.1186/s40623-015-0246-7>.
- 500 Abdu, M.A.,(2001), Outstanding problems in the equatorial iono-
 501 sphere–thermosphere electrodynamics relevant to Spread-F, *Journal of Atmo-*
 502 *spheric and Solar-Terrestrial Physics*, Volume 63, Issue 9, 2001, PP: 869-884,
 503 ISSN 1364-6826, [https://doi.org/10.1016/S1364-6826\(00\)00201-7](https://doi.org/10.1016/S1364-6826(00)00201-7).
- 504 Abdullah, S., Arief, A., and Muhammad, M., (2018). Utilization of NVIS HF Radio
 505 As Alternative Technologies In Rural Area of North Maluku. *Proceedings of*
 506 *the International Conference on Science and Technology, ICST*, pp. 734–39.
 507 doi: 10.2991/icst-18.2018.149.
- 508 Ads, A. G., P. Bergada, J. R. Regué, R. M. Alsina-Pagès, J. L. Pijoan, D. Altadill,
 509 D. Badia, and S. Graells. (2015), Vertical and Oblique Ionospheric Sound-
 510 ings over the Long Haul HF Link between Antarctica and Spain, *Radio Sci-*
 511 *ence*,50(9):916–30. doi: 10.1002/2015RS005773.
- 512 Andersen, J. B., Rappaport, T. S., and Yoshida, S., (1995) Propagation measure-
 513 ments and models for wireless communications channels, *IEEE Communica-*
 514 *tions Magazine*, vol. 33, no. 1, pp. 42-49, Jan. 1995, doi: 10.1109/35.339880.
- 515 Angling, J., Matthew, S., Paul Cannon, C., Nigel Davies, J. Tricia Willink, Vi-
 516 vianne Jodalen, and Bengt Lundborg. (1998), Measurements of Doppler and

- 517 Multipath Spread on Oblique High-Latitude HF Paths and Their Use in Char-
 518 acterizing Data Modem Performance. *Radio Science*, 33(1):97–107.
- 519 Bergadà, P., J. L. Pijoan, M. Salvador, J. R. Regué, D. Badia, and S. Graells.
 520 (2014), Digital Transmission Techniques for a Long Haul HF Link: DSSS
 521 versus OFDM, *Radio Science*, 518–30. doi: 10.1002/2013RS005203.1.
- 522 Bole, A., Wall, A., and Norris A, (2014), Chapter 2 - The Radar System – Tech-
 523 nical Principles, Radar and ARPA Manual (Third Edition), (Butterworth-
 524 Heinemann, PP: 29-137, ISBN 9780080977522, [https://doi.org/10.1016/B978-](https://doi.org/10.1016/B978-0-08-097752-2.00002-7)
 525 [0-08-097752-2.00002-7](https://doi.org/10.1016/B978-0-08-097752-2.00002-7).
- 526 Chen, G., Zhao, Z., Zhu, G., Huang, Y., and Li, T., (2010), HF Radio-Frequency
 527 Interference Mitigation, (*IEEE Geoscience and Remote Sensing Letters*, Vol. 7,
 528 no. 3, pp. 479-482, July 2010, doi: 10.1109/LGRS.2009.2039340.
- 529 Commonwealth of Australia, Bureau of Meteorology, (2023), *ASAPS*. Retrieved
 530 from: <https://www.sws.bom.gov.au/ProductsandServices/1/2>
- 531 Cox, Donald C. (1972) , Delay Doppler Characteristics of Multipath Propagation
 532 at 910 Mhz in a Suburban Mobile Radio Environment, *IEEE Transactions on*
 533 *Antennas and Propagation* 20(5):625–35. doi: 10.1109/TAP.1972.1140277.
- 534 Davies, K. (1965), Ionospheric radio propagation (Vol. 80). *US Department of Com-*
 535 *merce, National Bureau of Standards*.
- 536 Drongowski (2020): *Ham It Up Upconverter*. Retrieve from:
 537 [https://support.noolec.com/hc/en-us/articles/360005812474-Ham-It-Up-](https://support.noolec.com/hc/en-us/articles/360005812474-Ham-It-Up-Upconverter)
 538 [Upconverter](https://support.noolec.com/hc/en-us/articles/360005812474-Ham-It-Up-Upconverter).
- 539 Duncan, R., A. (1960), The equatorial F-region of the ionosphere, *Journal of At-*
 540 *mospheric and Terrestrial Physics*, Volume 18, Issues 2–3, 89-100, ISSN 0021-
 541 9169, [https://doi.org/10.1016/0021-9169\(60\)90081-7](https://doi.org/10.1016/0021-9169(60)90081-7).
- 542 Eliardsson, P., Axell, E., Stenumgaard, P., Wiklundh, K., Johansson, B., and B.
 543 Asp (2015), Military HF communications considering unintentional platform-
 544 generated electromagnetic interference, *Proceeding 2015 International Confer-*
 545 *ence on Military Communications and Information Systems (ICMCIS)*, 1-6,
 546 doi: 10.1109/ICMCIS.2015.7158700.
- 547 Goodman (2005). The Ionosphere. In: Space Weather Telecommunications. *The*
 548 *International Series in Engineering and Computer Science*, vol 782. Springer,
 549 Boston, MA. <https://doi.org/10.1007/0-387-23671-63>
- 550 Goldsmith, A (2005), Wireless Communications, *Cambridge University Press* p. 86,
 551 ISBN 978-0-521-83716-3
- 552 Great Scott Gadgets (2021), *FAQ: What is the Transmit Power of HackRF?*. Re-
 553 trieved from <https://hackrf.readthedocs.io/en/latest/faq.html>
- 554 HB9JAG, (2013), *Some Measurements on DVB-T Dongles with E4000 and*
 555 *R820T Tuners: Image Rejection, Internal Signals, Sensitivity, Overload,*
 556 *1dB Compression, Intermodulation,*. Retrieved from [https://www.rtl-](https://www.rtl-sdr.com/measurements-on-rtl-sdr-e4000-and-r820t-dvb-t-dongles-image-rejection-internal-signals-sensitivity-overload-1db-compression-intermodulation/)
 557 [sdr.com/measurements-on-rtl-sdr-e4000-and-r820t-dvb-t-dongles-image-](https://www.rtl-sdr.com/measurements-on-rtl-sdr-e4000-and-r820t-dvb-t-dongles-image-rejection-internal-signals-sensitivity-overload-1db-compression-intermodulation/)
 558 [rejection-internal-signals-sensitivity-overload-1db-compression-intermodulation/](https://www.rtl-sdr.com/measurements-on-rtl-sdr-e4000-and-r820t-dvb-t-dongles-image-rejection-internal-signals-sensitivity-overload-1db-compression-intermodulation/)
- 559 Helmholtz Centre Potsdam German Research Centre for Geosciences GFZ (2023)
 560 (Kp-Index. Retrieved from: <https://kp.gfz-potsdam.de/en/data>
- 561 Icom Inc.,(2015), *ICOM IC-718 Instruction Book*. Retrieved from
 562 <https://www.icomjapan.com/support/manual/1427/>
- 563 International Telecommunication Union (2000), *Recommendation ITU-R Rec.*
 564 *F.1487. Testing of HF modems with bandwidths of up to about 12 kHz using*
 565 *ionospheric channel simulators*. Retrieved from [https://www.itu.int/rec/R-](https://www.itu.int/rec/R-REC-F.1487-0-200005-I/en)
 566 [REC-F.1487-0-200005-I/en](https://www.itu.int/rec/R-REC-F.1487-0-200005-I/en)
- 567 Jiyo, (2013)., Analysis of Radio Wave Propagation Over Pameungpeuk-Bandung
 568 District Communication Circuit and Its Relations With Condition of Iono-
 569 sphere, *Jurnal Sains Dirgantara*, Vol. 11, no. 1, pp. 29-40.
- 570 Kitano, T.,Tomioka, Y., Subekti, A., Sadiq, M. A., Juzoji, H., and Nakajima,
 571 I.,(2006), A basic study of the near vertical inclined skywave the last sur-

- vival tool of radio communications to support telemedicine after n-disaster, *HEALTHCOM 2006 8th International Conference on e-Health Networking, Applications and Services*, pp. 165-169, doi: 10.1109/HEALTH.2006.246440
- Kurniawati, I, Hendranto, G., and Taufik M, (2018) Statistical Modeling of Low-Latitude Long-Distance HF Ionospheric Multi-Mode Channels. *Progress in Electromagnetic Research Vol. 64*, PP:77–86. doi: doi:10.2528/PIERM17101603.
- Laufer, C., (2014), *The Hobbyist’s Guide to the RTL-SDR: Really Cheap Software Defined Radio: Kindle Edition*. RTL-SDR.com
- Maruyama, T. and Kawamura, M.(2006), Equatorial ionospheric disturbance observed through a transequatorial HF propagation experiment, *Ann. Geophys.*, 24, 1401–1409, <https://doi.org/10.5194/angeo-24-1401-2006>.
- Maslin, N.M. (1988), *HF Communications: A Systems Approach (1st ed.)*. CRC Press., <https://doi.org/10.4324/9780203168899>
- Matzka, Jürgen; Bronkalla, Oliver; Tornow, Katrin; Elger, Kirsten; Stolle, Claudia (2021): *Geomagnetic Kp index. V. 1.0*. GFZ Data Services. <https://doi.org/10.5880/Kp.0001>
- McNamara, L., F., (1991), *The Ionosphere: Communications, Surveillance, and Direction Finding*, *Kruger Pub. Co.*, Malabar, 1991.
- Murugan, M., Purandare R., G., and Tavildar A., S., (2008), Near Vertical Incidence Skywave (NVIS) Propagation. *Proceedings of the international conference on sensors, signal processing, communication, control and instrumentation (SSPCCIN) January 3-5, VIT Pune, India*
- Munro, G. H. (1953). Reflexions from irregularities in the ionosphere. *Proceedings of the Royal Society of London A*, 219, 447–463.
- Munro, G. H., Heisler, L. H. (1958). Ionospheric records of solar eclipses. *Journal of Atmospheric and Solar-Terrestrial Physics*, 12, 57–67.
- Namboothiri, S. P., Balan, N., and Rao, P. B. (1989), Vertical plasma drifts in the F region at the magnetic equator, *J. Geophys. Res.*, 94(A9), 12055– 12060, doi:10.1029/JA094iA09p12055.
- Ossmann, M., (2016), *Software defined radio with HackRF*. Retrieved from: <https://greatscottgadgets.com/sdr>
- Pirkel, Ryan J., and Gregory D. Durgin. (2008), Optimal Sliding Correlator Channel Sounder Design, *IEEE Transactions on Wireless Communications* 7(9):3488–97. doi: 10.1109/TWC.2008.070278.
- Porte, J., Maso, J. Pijoan, J., Miret, M., Badia, D., and Jayasinghe, J., (2018) Education and e-health for developing countries using NVIS communications, *2018 IEEE Region 10 Humanitarian Technology Conference (R10-HTC)*, pp. 1-5, doi: 10.1109/R10-HTC.2018.8629842.
- Salous, S., (2013), *Radio Propagation Measurement and Channel Modelling*, 1st ed., Wiley, 2013, pp.182-191.
- Suksmono, A., B., (2013), A Simple Solution to the Uncertain Delay Problem in USRP Based SDR-Radar Systems, *arXiv 1309.4843*, pp. 1-4, 2013
- Ulversoy, T., (2010), Software Defined Radio: Challenges and Opportunities, *IEEE Communications Surveys Tutorials*, vol. 12, no. 4, pp. 531-550, Fourth Quarter 2010, doi: 10.1109/SURV.2010.032910.00019.
- Wang, J., Ding, G., and Wang, H. (2018). HF Communications: Past, Present, and Future. *China Communications*, 15, 1–9
- Withington, T. (2020, June 10). *HF Radio: Still Valid After 100 Years*. Retrieved from <https://www.asianmilitaryreview.com/2020/06/hf-radio-still-valid-after-100-years>
- World Data Center for Geomagnetism, Kyoto, M. Nose, T. Iyemori, M. Sugiura, T. Kamei (2015), *Geomagnetic Dst index*, doi:10.17593/14515-74000